Article

Cell Reports

Microglia Are Indispensable for Synaptic Plasticity in the Spinal Dorsal Horn and Chronic Pain

Graphical Abstract

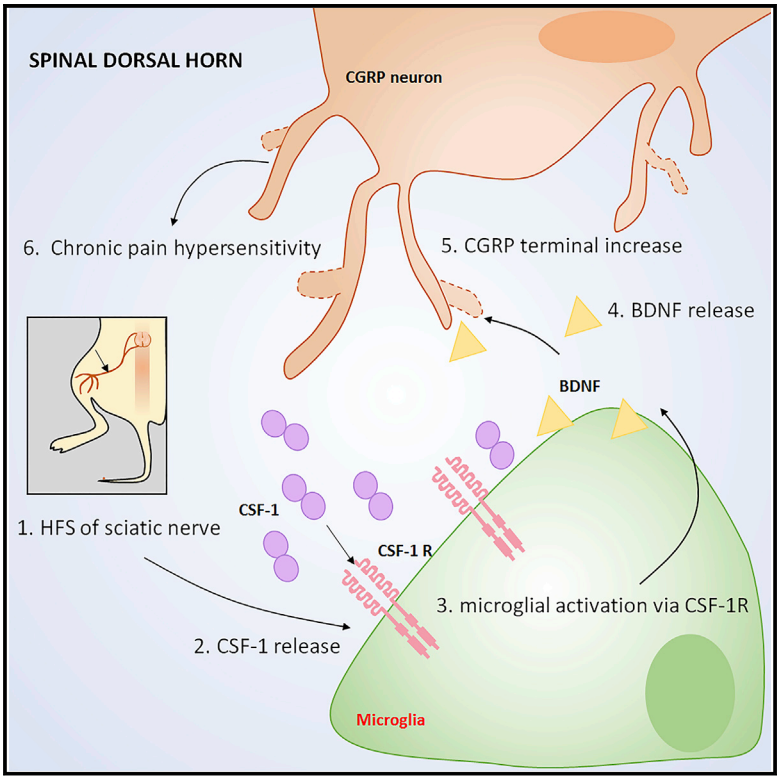

Highlights

- HFS triggers synaptic plasticity of CGRP afferents and chronic pain
- LTP-inducible HFS activates spinal microglia through CSF1 signaling
- Microglial BDNF is essential for HFS-induced spinal LTP and chronic pain

Authors

Li-Jun Zhou, Jiyun Peng, Ya-Nan Xu, ..., Zhi Tan, Xian-Guo Liu, Long-Jun Wu

Correspondence

tanzhi@mail.sysu.edu.cn (Z.T.), liuxg@mail.sysu.edu.cn (X.-G.L.), wu.longjun@mayo.edu (L.-J.W.)

In Brief

Zhou et al. characterize chronic pain behaviors triggered by LTP-inducible HFS without nerve injury. They identify that HFS-induced LTP is accompanied by an increase in CGRP terminals in the spinal dorsal horn. Activation of neuronal CSF1-microglial BDNF signaling is indispensable for the synaptic and structural plasticity underlying HFS-induced chronic pain.

Zhou et al., 2019, Cell Reports *27*, 3844–3859
June 25, 2019
https://doi.org/10.1016/j.celrep.2019.05.087

CellPress

OPEN ACCESS
CellPress

Cell Reports
Article

Microglia Are Indispensable for Synaptic Plasticity in the Spinal Dorsal Horn and Chronic Pain

Li-Jun Zhou,[1,2,3,11] Jiyun Peng,[2,4,11] Ya-Nan Xu,[1] Wei-Jie Zeng,[1] Jun Zhang,[1] Xiao Wei,[1] Chun-Lin Mai,[1] Zhen-Jia Lin,[1] Yong Liu,[2,4] Madhuvika Murugan,[2,4] Ukpong B. Eyo,[2,4] Anthony D. Umpierre,[4] Wen-Jun Xin,[1,3] Tao Chen,[5] Mingtao Li,[3] Hui Wang,[6,7] Jason R. Richardson,[8] Zhi Tan,[1,*] Xian-Guo Liu,[1,3,*] and Long-Jun Wu[2,4,9,10,12,*]

[1]Department of Physiology and Pain Research Center, Zhongshan School of Medicine, Sun Yat-sen University, Guangzhou 510080, China
[2]Department of Cell Biology and Neuroscience, Rutgers University, Piscataway, NJ 08854, USA
[3]Guangdong Province Key Laboratory of Brain Function and Disease, Guangzhou 510080, China
[4]Department of Neurology, Mayo Clinic, Rochester, MN 55905, USA
[5]Department of Anatomy, Histology and Embryology and K.K. Leung Brain Research Center, the Fourth Military Medical University, Xi'an 710032, China
[6]Department of Neuroscience and Cell Biology, Rutgers-Robert Wood Johnson Medical School, Piscataway, NJ 08854, USA
[7]Department of Pharmacology, School of Pharmacy, Nantong University, Nantong 22600, China
[8]Departments of Environmental Health Sciences, Florida International University, Miami, FL 33199, USA
[9]Department of Neuroscience, Mayo Clinic, Jacksonville, FL 32224, USA
[10]Department of Immunology, Mayo Clinic, Rochester, MN 55905, USA
[11]These authors contributed equally
[12]Lead Contact
*Correspondence: tanzhi@mail.sysu.edu.cn (Z.T.), liuxg@mail.sysu.edu.cn (X.-G.L.), wu.longjun@mayo.edu (L.-J.W.)
https://doi.org/10.1016/j.celrep.2019.05.087

SUMMARY

Spinal long-term potentiation (LTP) at C-fiber synapses is hypothesized to underlie chronic pain. However, a causal link between spinal LTP and chronic pain is still lacking. Here, we report that high-frequency stimulation (HFS; 100 Hz, 10 V) of the mouse sciatic nerve reliably induces spinal LTP without causing nerve injury. LTP-inducible stimulation triggers chronic pain lasting for more than 35 days and increases the number of calcitonin gene-related peptide (CGRP) terminals in the spinal dorsal horn. The behavioral and morphological changes can be prevented by blocking NMDA receptors, ablating spinal microglia, or conditionally deleting microglial brain-derived neurotrophic factor (BDNF). HFS-induced spinal LTP, microglial activation, and upregulation of BDNF are inhibited by antibodies against colony-stimulating factor 1 (CSF-1). Together, our results show that microglial CSF1 and BDNF signaling are indispensable for spinal LTP and chronic pain. The microglia-dependent transition of synaptic potentiation to structural alterations in pain pathways may underlie pain chronicity.

INTRODUCTION

Chronic pain manifests as allodynia (decreased pain threshold), hyperalgesia (increased pain response), and spontaneous pain. Chronic pain affects about 20% of the population and results in significant expenditure of healthcare resources (Yekkirala et al., 2017). The main mechanisms underlying pathological pain include hypersensitivity of nociceptors and persistent increases in synaptic transmission within pain pathways (Liu and Zhou, 2015). However, because conditions that induce chronic pain are often associated with peripheral nerve degeneration and local inflammation, it is not clear whether persistent synaptic potentiation alone is sufficient to result in chronic pain.

Long-term potentiation (LTP) at C-fiber synapses in the spinal dorsal horn (SDH) induced by high-frequency stimulation (HFS) of the peripheral nerve is considered a synaptic model of pathological pain (Liu and Zhou, 2015). Indeed, spinal LTP and nerve injury-induced neuropathic pain share many common mechanisms (Sandkühler and Gruber-Schoffnegger, 2012). In particular, both depend on N-methyl-D-aspartic acid (NMDA) receptors (Liu and Sandkühler, 1995; Seltzer et al., 1991). In human volunteers, HFS at skin nociceptors has been shown to produce mechanical allodynia and secondary hyperalgesia lasting for hours or even days in some cases (Pfau et al., 2011). In rats, HFS (0.5 ms, 40 V, 10 trains of 2 s at 100 Hz with 10-s intervals) at the sciatic nerve produces mechanical allodynia persisting for at least 35 days but also damages the stimulated nerve (Liang et al., 2010). To date, evidence of a causal link between spinal LTP and chronic pain is still lacking.

In response to peripheral nerve injury or inflammation, microglia, the principal immune cells, transform from a ramified to a reactive state and release a repertoire of proinflammatory factors that lead to pain hypersensitivity (Gu et al., 2016; Inoue and Tsuda, 2018; Peng et al., 2016; Zhuo et al., 2011). Several studies have shown that microglial activation is involved in HFS-induced LTP and can even regulate synaptic strength independent of neuronal activity (Clark et al., 2015; Gruber-Schoffnegger et al., 2013; Kronschläger et al., 2016; Zhong et al., 2010). However, it is still unclear whether microglia participate in spinal plasticity and pain hypersensitivity in the absence of nerve injury.

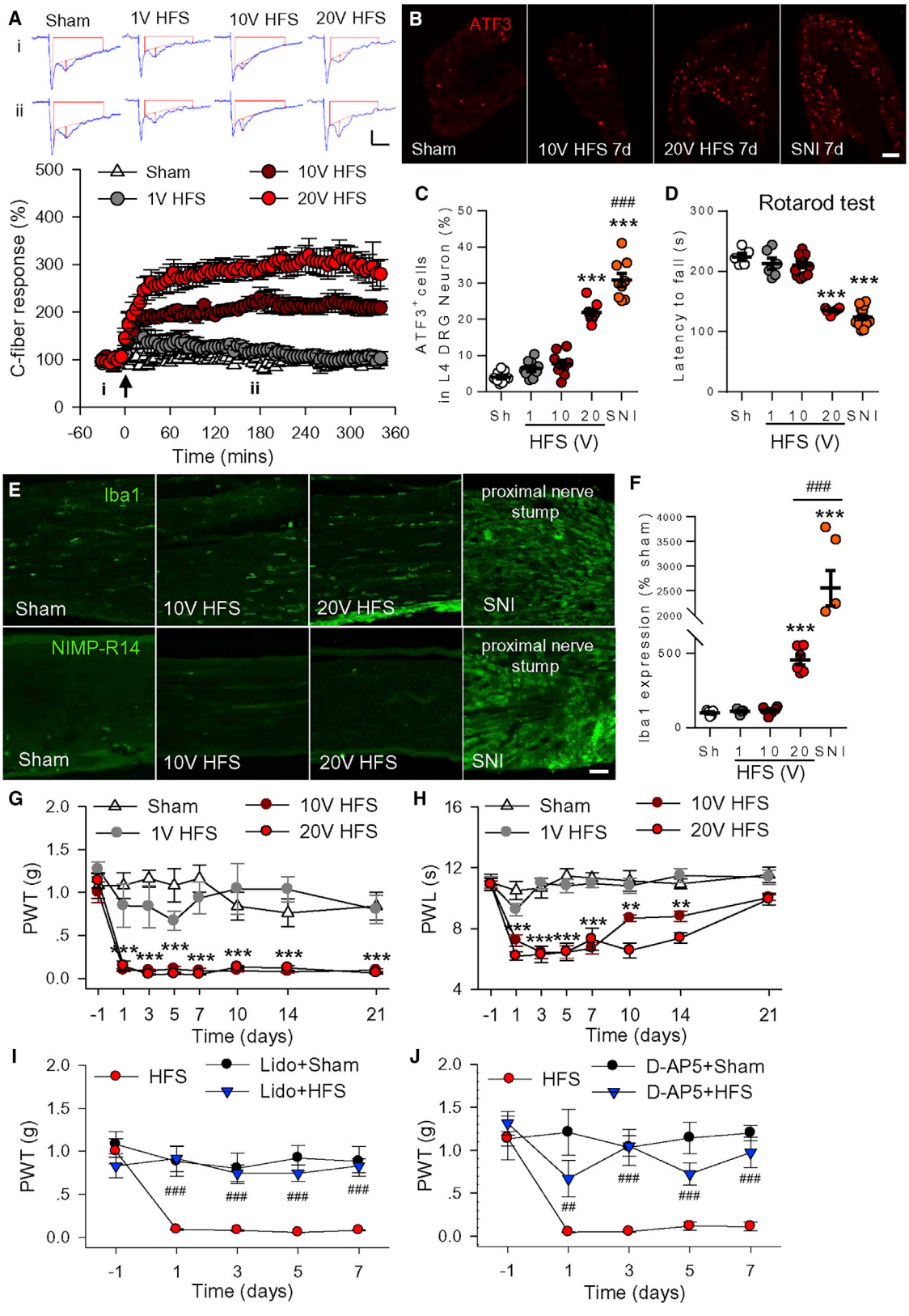

(legend on next page)

In the present study, we report that induction of spinal LTP at C-fiber synapses by HFS does not injure the stimulated nerve and leads to long-lasting mechanical allodynia and thermal hyperalgesia in mice. Using transgenic mice to either genetically ablate microglia or specifically knock out microglial BDNF, we determined that HFS at the sciatic nerve activates spinal microglia via colony-stimulating factor 1 (CSF-1; namely, macrophage CSF) signaling, which, in turn, releases BDNF from microglia to increase calcitonin gene-related peptide (CGRP) terminals in the SDH. Increases in CGRP terminals underlie long-lasting pain hypersensitivity. These findings may explain how chronic pain occurs in the absence of injury or disease, a state recently classified as chronic primary pain by the World Health Organization (Treede et al., 2015).

RESULTS

HFS Induces Chronic Pain without Detectable Injury of the Stimulated Nerve

It has been proposed that spinal LTP at C-fiber synapses, induced by HFS, may underlie chronic pain (Liu and Zhou, 2015). However, HFS may also induce chronic pain through injury of the stimulated nerve (Liang et al., 2010). To explore the causal relationship between spinal LTP and chronic pain, a certain stimulation protocol that reliably induces LTP but does not damage the stimulated nerve was first characterized. To this end, we modulated the intensity of HFS and examined the corresponding changes in spinal LTP induction and potential nerve damage in mice. We found that HFS (100 pulses of 0.5 ms at 100 Hz, repeated 4 times at 10-s intervals) of the sciatic nerve at both 10 V and 20 V, but not at 1 V, induced LTP of C-fiber-evoked field postsynaptic excitatory potentials (fEPSPs) (Figure 1A). To determine whether the stimulation protocols may damage sensory neurons, we performed immunofluorescence analysis to detect ATF3-positive nuclei, a well-established injury marker, in L4 dorsal root ganglia (DRGs) after electrical stimulation. ATF3 was significantly increased in mice receiving 20 V HFS or spared nerve injury (SNI) surgery. However, neither 10 V nor 1 V of HFS caused ATF3 upregulation (Figures 1B and 1C). Compared with the sham group, the latencies to fall in the rotarod test, which evaluates motor function, was significantly decreased in the 20 V HFS and SNI groups 7 days after surgery but not in the 10 V HFS group (Figure 1D). Because subtle damage to the nerve may attract pro-nociceptive immune cells, we examined resident macrophages (stained by Iba1) and neutrophils (by NIMP-R14) in 10 V HFS-stimulated sciatic nerve 7 days after HFS. Compared with the sham group, there was no significant change in Iba1 in stimulated sciatic nerves (Figures 1E and 1F). NIMP-R14 neutrophils were not detected in the sham and HFS groups. In contrast, these immune cells were activated or infiltrated in the proximal sciatic nerve stump or the connective tissue in SNI mice. Together, these results indicate that 10 V HFS induces spinal LTP but does not result in injury or inflammation in the stimulated nerve.

To determine whether HFS is capable of inducing chronic pain, behavioral tests were performed in mice receiving HFS at different intensities. Compared with the sham control, HFS at 20 V and 10 V, but not at 1 V, led to a reduction in paw withdrawal threshold (PWT) with mechanical stimuli (mechanical allodynia) (Figure 1G) and in paw withdrawal latency (PWL) with thermal stimuli (thermal hyperalgesia) (Figure 1H). The mechanical allodynia and the thermal hyperalgesia induced by 10 V HFS lasted for more than 21 days and around 14 days, respectively.

HFS may induce numerous changes in the stimulated nerve. To rule out other changes that may contribute to chronic pain hypersensitivity, we blocked action potential conduction in the sciatic nerve with lidocaine (a sodium channel blocker, 2%, 50 μL) 15 min before HFS and found that mechanical allodynia was completely blocked (Figure 1I). Spinal LTP is NMDA receptor-dependent (Liu and Sandkühler, 1995). We found that intrathecal injection of the NMDA receptor antagonist D-AP5 (50 μg/mL, 5 μL, 253 nM) blocked spinal LTP without affecting the C-fiber-evoked fEPSP baseline (Figure S1).This, in turn, prevented HFS-induced allodynia (antagonist applied 30 min before 10 V HFS; Figure 1J). These results indicate that spinal LTP is responsible for chronic pain hypersensitivity.

We repeated the above HFS experiments in rats, a species also commonly used to test chronic pain. Interestingly, we found

Figure 1. HFS that Does Not Injure the Stimulated Sciatic Nerve Induces Spinal LTP and Chronic Pain Hypersensitivity in Mice

(A) Spinal LTP at C-fiber synapses was induced by HFS at 10 and 20 V but not at 1 V. The representative traces of C-fiber evoked fEPSPs were recorded before (i) and 3 h (ii) after high-frequency stimulation (HFS) of the sciatic nerve at different intensities. The amplitude of C-fiber-evoked fEPSPs (red vertical line) was determined automatically by the parameter extraction software WinLTP. Scale bars, 100 ms (x) and 0.2 mV (y). Summary data of the C-fiber responses expressed as mean ± SEM plotted versus time are shown below (n = 6 mice/group). The arrow indicates the time point when HFS was delivered.

(B and C) Representative images (B) and statistical data (C) showing the expression of ATF3 in L4 DRG neurons 7 days after HFS at different intensities and 7 days after spared nerve injury (SNI). Scale bar, 100 μm. n = 3–4 mice/group, 3 slices/mouse; ***$p < 0.001$ compared with the sham group, $^{###}p < 0.001$ versus 20 V HFS; one-way ANOVA with Tukey's test.

(D) The latencies to fall in the rotarod test in different groups 7 days after HFS at different intensities or SNI. n = 5–12 mice for each group, ***$p < 0.001$ compared with the sham group, one-way ANOVA with Tukey's test.

(E) Immunofluorescence of Iba1 (a marker of resident macrophages) and NIMP-R14 (a marker of neutrophils) in the stimulated sciatic nerve from different groups 7 days after HFS or SNI (n = 3 mice/group, 2–3 sections/mouse). Scale bar, 50 μm.

(F) Quantification of Iba1 expression in the sciatic nerve. ***$p < 0.001$ compared with the sham group, $^{###}p < 0.001$ versus 20 V HFS; one-way ANOVA with Tukey's test.

(G and H) HFS at 10 V and 20 V significantly decreased the 50% paw withdrawal threshold (PWT) (G) to von Frey filaments and paw withdrawal latency (PWL) (H) to radiant thermal stimuli compared with the sham group or 1 V HFS (n = 12 mice for the 10 V HFS group, n = 5–6 mice for other groups; **$p < 0.01$, ***$p < 0.001$ versus the sham group; two-way ANOVA with Fisher's least significant difference [LSD] test).

(I) The decrease in mechanical thresholds induced by 10 V HFS was prevented by local application of 2% lidocaine (50 μL) at the stimulated sciatic nerve 15 min before HFS (n = 5–7 mice/group). $^{###}p < 0.001$ versus the HFS group, two-way ANOVA with Fisher's LSD's test.

(J) Intrathecal injection of the NMDA receptor antagonist D-AP5 (50 μg/mL, 5 μL) but not vehicle (Vehi, PBS) 30 min before HFS abolished HFS-induced mechanical hypersensitivity (n = 6–8 mice/group). $^{##}p < 0.01$, $^{###}p < 0.001$ versus the Vehi group; two-way ANOVA with Fisher's LSD's test.

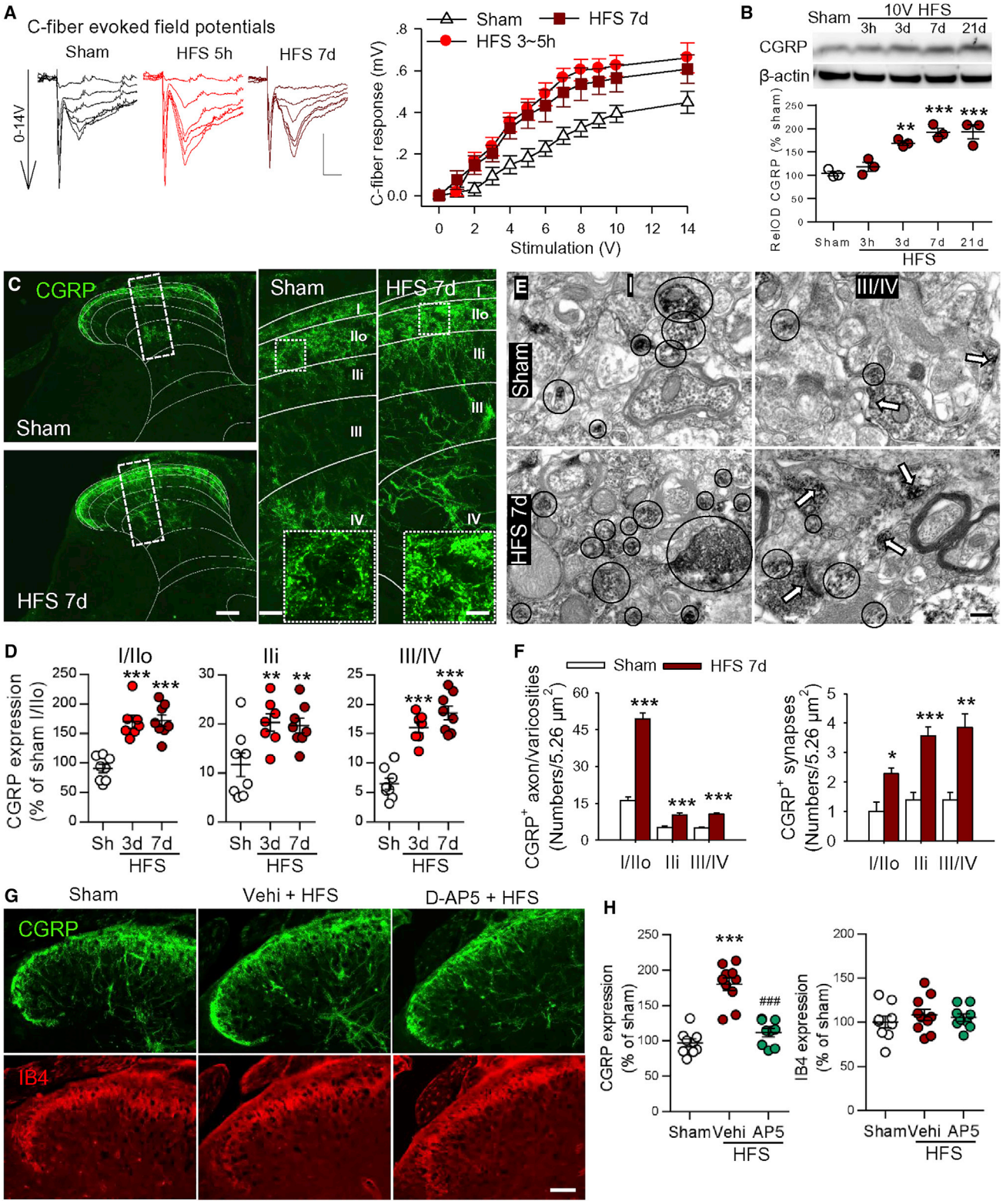

Figure 2. HFS Induces Long-Lasting Synaptic Potentiation and Enhances CGRP Terminals in the SDH in a NMDA Receptor-Dependent Manner

(A) Original representative traces of fEPSP and the input and output curves (stimulation intensity and C-fiber response) demonstrated that synaptic efficacy was enhanced at 3–5 h or 7–14 days after 10 V HFS (n = 12 mice in the sham and HFS 3–5 h groups, n = 8 mice in the HFS 7- to 14-day group; two-way ANOVA with Tukey's test). Scale bars, 50 ms (x) and 0.2 mV (y).

(legend continued on next page)

that 20 V HFS at the rat sciatic nerve did not induce nerve injury (no ATF3 upregulation) but was able to induce spinal LTP as well as chronic pain hypersensitivity (Figures S2A–S2D). Histological analyses using transmission electron microscopy (TEM) indicated that, unlike SNI, electrical stimulation of the rat sciatic nerve at 20 V HFS did not induce Wallerian degeneration of myelinated nerve fibers and atrophy of axons in myelinated and unmyelinated nerve fibers (Figures S2E and S2F). Taken together, HFS-induced spinal LTP alone without nerve damage is sufficient to trigger chronic pain hypersensitivity in mice and rats. In further experiments, we investigated the cellular and molecular mechanisms by which spinal LTP underlies chronic allodynia using pharmacological and genetic tools and the 10 V HFS stimulation protocol.

10 V HFS Induces Long-Lasting Functional and Structural Plasticity in the SDH

To address the cellular mechanism underlying the long-lasting allodynia induced by short (4-s) electrical stimulation, we investigated the possibility of functional and structural plasticity in the SDH after 10V HFS. To determine whether 10 V HFS induces long-lasting LTP, we investigated the input and output curves of C-fiber fEPSPs in mice receiving HFS 3–5 h or 7–14 days before recordings and found that the curves shifted left in both groups compared with sham mice (Figure 2A). The data indicate that the spinal LTP induced by 10 V HFS in mice can persist for more than 2 weeks.

To investigate the structural bases of the long-lasting synaptic potentiation initiated by 10 V HFS, the CGRP$^+$ peptidergic and IB4$^+$ nonpeptidergic C-fiber terminals in the dorsal horn were examined following 10 V HFS. Western blots showed that CGRP was significantly upregulated 3 days after HFS and that the change persisted for more than 21 days (Figure 2B). Immunohistochemical experiments showed that CGRP$^+$ terminals in the SDH were mainly located in lamina I and outer lamina II (IIo) in sham control mice. However, in mice treated with HFS, the CGRP$^+$ terminals were dramatically increased in both superficial and deep laminae of the SDH (Figures 2C and 2D). Serial spinal coronal sections showed that, 7 days after HFS, CGRP expression was markedly upregulated in the ipsilateral L4–L6 SDH, where sciatic nerve roots carry sensory input. Furthermore, the upregulation of CGRP was also extended to the ipsilateral L3 and S1 SDH (Figure S3).

Because the peptidergic terminals communicate with dorsal horn neurons by both volume transmission (via release of bioactive substances from varicosities) and by classical synaptic transmission (Borroto-Escuela et al., 2015), we employed pre-embedding immunoelectron microscopy (IEM) to test for changes in CGRP$^+$ varicosities and synapse numbers in the SDH. We found that both synapse number and varicosity were increased in lamina I–IV 7 days after HFS compared with the sham group (Figures 2E and 2F). Importantly, we found that, like LTP and chronic pain hypersensitivity, the increase in CGRP afferents induced by HFS was also prevented by intrathecal injection of the NMDA receptor antagonist D-AP5 (Figures 2G and 2H). In contrast, no change in IB4 expression was observed 7 days after HFS (Figures 2G and 2H).

Furthermore, immunostaining of the ipsilateral SDH showed that the fluorescence intensity of synaptophysin (a marker of presynaptic termini), GAP43 (a protein crucial for nerve fiber growth and sprouting; Benowitz and Routtenberg, 1997), and substance P (SP) were significantly increased 7 days after HFS compared with the sham group. Their colocalization with CGRP was also increased (Figures S4A–S4E). Therefore, presynaptic synaptophysin, SP, and GAP43 levels are increased in CGRP$^+$ terminals after 10 V HFS. In addition, we found that the fluorescence intensity of CGRP in the cell bodies of ipsilateral L4 DRG neurons increases gradually from day 1 to day 7 after HFS (Figures S4F and S4G). HFS induces a long-lasting increase in CGRP terminals in the SDH, which may serve as a structural basis for chronic pain hypersensitivity induced by HFS.

Microglia Are Required for HFS-Induced LTP and Chronic Pain

Activation of microglia is important for both neuropathic pain induced by nerve injury (Inoue and Tsuda, 2018) and for LTP at C-fiber synapses (Clark et al., 2015). To determine the roles of microglia in 10 V HFS-induced synaptic plasticity and pain hypersensitivity, we first examined whether our stimulation protocol was able to activate spinal microglia. The expression of Iba1 (a marker of microglia) in the SDH was significantly upregulated at 3, 7, and 21 days but not acutely (5 h after HFS; Figure 3A). However, Iba1 staining also suggests that microglial somata become enlarged between 5 h and 7 days after HFS (Figure 3B). Further, the number of Iba1$^+$ spinal microglia was markedly increased 1 day after HFS (Figures 3B and 3C). In contrast to SNI, which activated microglia in both the dorsal and ventral horn, 10 V HFS did so only in the dorsal horn (Figure S5A).

(B) Western blot assay illustrating the time course of changes in CGRP levels in the ipsilateral SDH following 10 V HFS (n = 3–4 mice/group). $^{**}p < 0.01$, $^{***}p < 0.001$ versus the sham group; one-way ANOVA with Fisher's LSD test.

(C) Representative confocal images of whole ipsilateral SDH (left) and magnified images (right) showing the distributions of CGRP$^+$ terminals 7 days after 10 V HFS or sham operation. The laminae of the SDH are indicated by white lines. Representative higher-magnification images from the dotted boxed regions in the larger images show CGRP$^+$ varicosities. Scale bars: 100 μm (left), 20 μm (right), 5 μm (right inset).

(D) Histograms showing the increased expression of CGRP$^+$ terminals in different laminae of the ipsilateral SDH 3 or 7 days after HFS (n = 3–4 mice/group, 2–3 sections/mouse). $^{**}p < 0.01$, $^{***}p < 0.001$ compared with the sham group; one-way ANOVA with Fisher's LSD test.

(E and F) Electron micrographs (E) and histograms (F) showing the CGRP-immunoreactive varicosities and synapses in the different laminae of the ipsilateral SDH in the sham (n = 2 mice, 2–3 micrographs/lamina/mouse) and HFS groups (n = 3 mice, 2–3 micrographs/lamina/mouse). The black circles indicate CGRP$^+$ varicosities and the white arrows CGRP$^+$ synapses pointing from the presynaptic to the postsynaptic membrane. Scale bar, 200 nm. $^{*}p < 0.05$, $^{**}p < 0.01$, $^{***}p < 0.001$ compared with the sham group; one-way ANOVA with Tukey's post hoc test.

(G and H) Representative images (G) and statistical data (H) showing the expression of CGRP (green) and IB4 (red) in the SDH 7 days after 10 V HFS with or without the NMDA antagonist D-AP5 (AP5). Scale bar, 50 μm (left). n = 3 mice/group, n = 3–4 images/mouse. $^{***}p < 0.001$ compared with the sham group, $^{###}p < 0.001$ versus the Vehi HFS group; one-way ANOVA with Tukey's post hoc test.

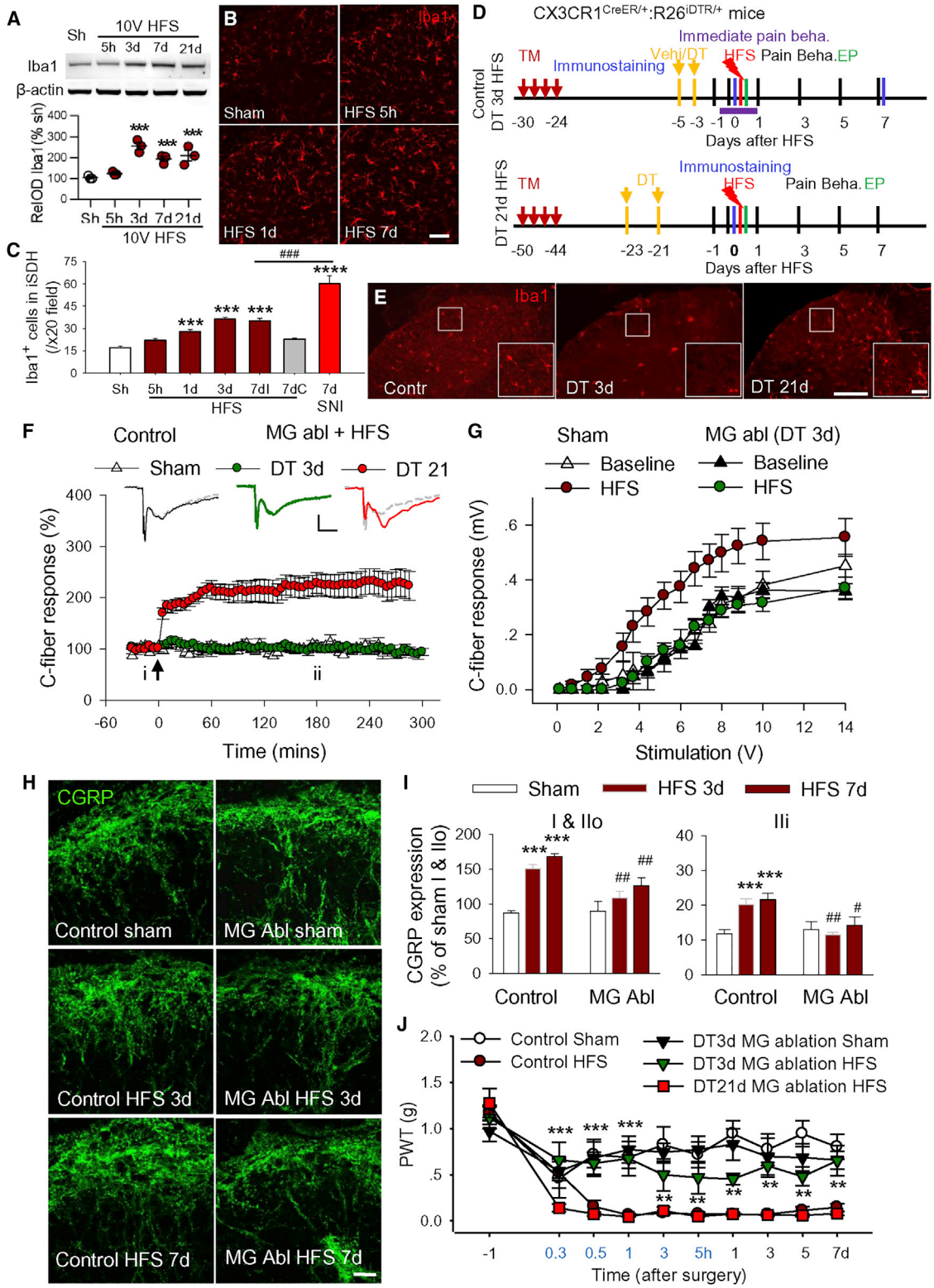

Figure 3. Microglia Ablation Blocks Spinal LTP, the Increase in CGRP Terminals, and Mechanical Allodynia Induced by HFS

(A) Western blots showing the time course of the Iba1 expression level after 10 V HFS (n = 3 mice/group). ***p < 0.001 versus the sham group, one-way ANOVA with Fisher's LSD test.

(legend continued on next page)

To determine the causal link between microglial activation, spinal plasticity, and chronic pain hypersensitivity, we performed experiments with CX3CR1$^{CreER/+}$:R26$^{iDTR/+}$ mice, in which CX3CR1 cells express the diphtheria toxin (DT) receptor (Parkhurst et al., 2013; Peng et al., 2016). DT was applied 3 weeks after the last injection of tamoxifen (TM) to selectively ablate microglia in the CNS but not peripheral macrophages because of their fast turnover. We found that microglia were largely ablated at 3 days after DT injection in CX3CR1CreER/+:R26iDTR/+ mice. Afterward, microglia fully repopulated within 3 weeks (Figures 3D and 3E). Interestingly, HFS at 10 V was unable to induce spinal LTP 3 days after DT injection, whereas LTP could be induced when microglia were repopulated 21 days after DT treatment (Figure 3F). These results strongly indicate that spinal microglia are required for HFS-induced LTP.

If microglial depletion abolishes LTP, then we expect that HFS-induced, long-lasting functional and structural plasticity would be reduced. Indeed, in mice receiving HFS 3 days after DT injection, fEPSP input and output curves, measured 7–14 days after HFS, were not different from sham mice. In non-DT control mice, HFS induced a leftward shift of the curve (Figure 3G). Consistently, the increase in CGRP terminals induced by HFS was also substantially attenuated in microglia-depleted mice compared with control mice (Figures 3H and 3I). Finally, we found that HFS-induced mechanical allodynia was significantly reduced in mice receiving a DT injection 3 days before HFS compared with either control mice or mice receiving a DT injection 21 days before HFS (Figure 4J). These results indicate that the development of mechanical allodynia is dependent on spinal microglia. Spinal LTP in mice was induced within 20 min after HFS and stabilized at around 1 (Figure 1A and 3F). We observed that mechanical hypersensitivity developed swiftly and fully 30 min after HFS (Figure 4J). To test whether microglia are also involved in the maintenance of mechanical allodynia, DT was injected 7 days and 9 days after HFS. We found that deletion of microglia was unable to reverse HFS-induced mechanical allodynia (Figures S5B and S5C). Together, these results suggest that microglia are indispensable for induction but not for maintenance of HFS-induced chronic pain hypersensitivity.

Microglial BDNF Is Essential for HFS-Induced LTP and Chronic Pain

BDNF has been implicated in spinal LTP and neuropathic pain (Coull et al., 2005; Zhou et al., 2011). Therefore, we examined the role of microglial BDNF in synaptic plasticity and chronic pain induced by HFS using CX3CR1$^{CreER/+}$:BDNF$^{flox/flox}$ male mice, in which BDNF can be specifically deleted from microglia by TM injection. To ensure deletion of microglial BDNF, the experiments were performed around 3 weeks after TM injection (Figure 4A). We found that HFS induced LTP and increased CGRP^{+} terminals in the SDH in control mice (BDNF$^{+/+}$) but not in mice with microglial BDNF deletion (BDNF$^{-/-}$; Figures 4A–4D). Deletion of BDNF from microglia attenuated HFS-induced mechanical allodynia in both male and female mice, whereas the same manipulation prevented SNI-induced pain hypersensitivity only in male mice (Figure 4E), which is consistent with a previous work (Sorge et al., 2015). These results indicate that microglial BDNF is required for HFS-induced functional and structural synaptic plasticity in the SDH, contributing to chronic pain.

To confirm the roles of BDNF for HFS-induced cellular and behavioral changes, BDNF (20 ng/μL, 5 μL) was injected intrathecally into wild-type mice. We found that BDNF directly caused mechanical allodynia that lasted for more than 10 days (Figure S6A). Consistent with the role of BDNF in promoting the sprouting of CGRP primary afferents (Orita et al., 2011; Song et al., 2008), immunostaining and western blot revealed that CGRP expression in the SDH was significantly increased 3 days after BDNF injection (Figures S6B and S6C), whereas CGRP in DRG neurons was not changed (data not shown). To further investigate the effect of BDNF on CGRP terminals and to explore the underlying mechanisms, we performed experiments in cultured DRG neurons. Compared with the control cultures, application of BDNF (50 ng/mL) for 1 day markedly increased CGRP neurite length. This effect of BDNF was abolished by both the tropomyosin receptor kinase B (TrkB) antagonist ANA-12 (10 μM) and the cAMP-response element binding protein (CREB) inhibitor 666-15 (0.5 μM) (Figures S6D and S6E). These results suggest that BDNF promotes the increase in CGRP terminals via the BDNF/TrkB/CREB signaling pathway.

(B and C) Representative images of Iba1 immunostaining (B) and histogram (C) showing that the number of Iba1^{+} microglia were increased in the ipsilateral SDH 1, 3, and 7 days after 10 V HFS and 7 days after SNI. Iba1^{+} cells were increased only in the ipsilateral but not in the contralateral SDH 7 days after HFS (7dI and 7dC). Scale bar, 50 μm. n = 3 mice/group, 2–3 sections/mouse. ***p < 0.001, ****p < 0.0001 versus the sham group, $^{###}$p < 0.001 versus the HFS 7-day group; one-way ANOVA with Fisher's LSD test.

(D) Experiment designs for control or microglial ablation (MG abl) 3 or 21 days after Vehi (corn oil) diphtheria toxin treatment in CX3CR1$^{CreER/+}$:R26$^{iDTR/+}$mice. DT, diphtheria toxin; TM, tamoxifen; Pain Beha, pain behavior test; EP, electrophysiology. In the DT 3-day HFS or DT 21-day HFS group, DT was injected 3 weeks after TM, and HFS was delivered 3 or 21 days after last application of DT. In the control group, Vehi but not DT was injected following TM injection.

(E) Immunofluorescent staining showing that microglia were largely depleted 3 days after DT treatment (DT 3d) and then fully repopulated within 21 days after DT treatment (DT 21d) in CX3CR1$^{CreER/+}$:R26$^{iDTR/+}$ mice. Boxed areas are magnified in the right panel. Scale bars, 100 μm (left) and 25 μm (right).

(F) HFS was able to induce LTP 21 days but not 3 days after DT injection (n = 12 mice for the DT 3-day group, n = 6–7 mice for the other groups; two-way ANOVA with Tukey's test). Representative traces of evoked C-fiber fEPSP are shown above before (i, gray line) and 3 h after 10 V HFS (ii, colored line). Scale bars, 100 ms (x) and 0.15 mV (y). The arrow indicates the time point when HFS was delivered.

(G) Input and output curves of fEPSPs measured 7 days after HFS in mice treated with DT (for MG abl) and with Vehi (n = 5 mice for the sham group, n = 5 or 7 mice for the MG abl groups).

(H and I) Representative images (H) and statistical analysis (I) showed the increase in CGRP^{+} terminals induced by HFS was substantially attenuated in microglia ablation mice (n = 3 mice/group, 2–3 sections/mouse). Scale bar, 20 μm. ***p < 0.001 versus the control sham group; $^{#}$p < 0.05, $^{##}$p < 0.01 versus the control HFS 3-day or 7-day group; one-way ANOVA with Fisher's LSD test.

(J) HFS induced mechanical allodynia in mice with microglia full repopulation (DT 21 days) but not in mice with microglia ablation (DT 3 days). n = 12 mice in the MG abl DT 3-day group, n = 8 mice for other groups. **p < 0.01, ***p < 0.001 versus control HFS; two-way ANOVA with Fisher's LSD test.

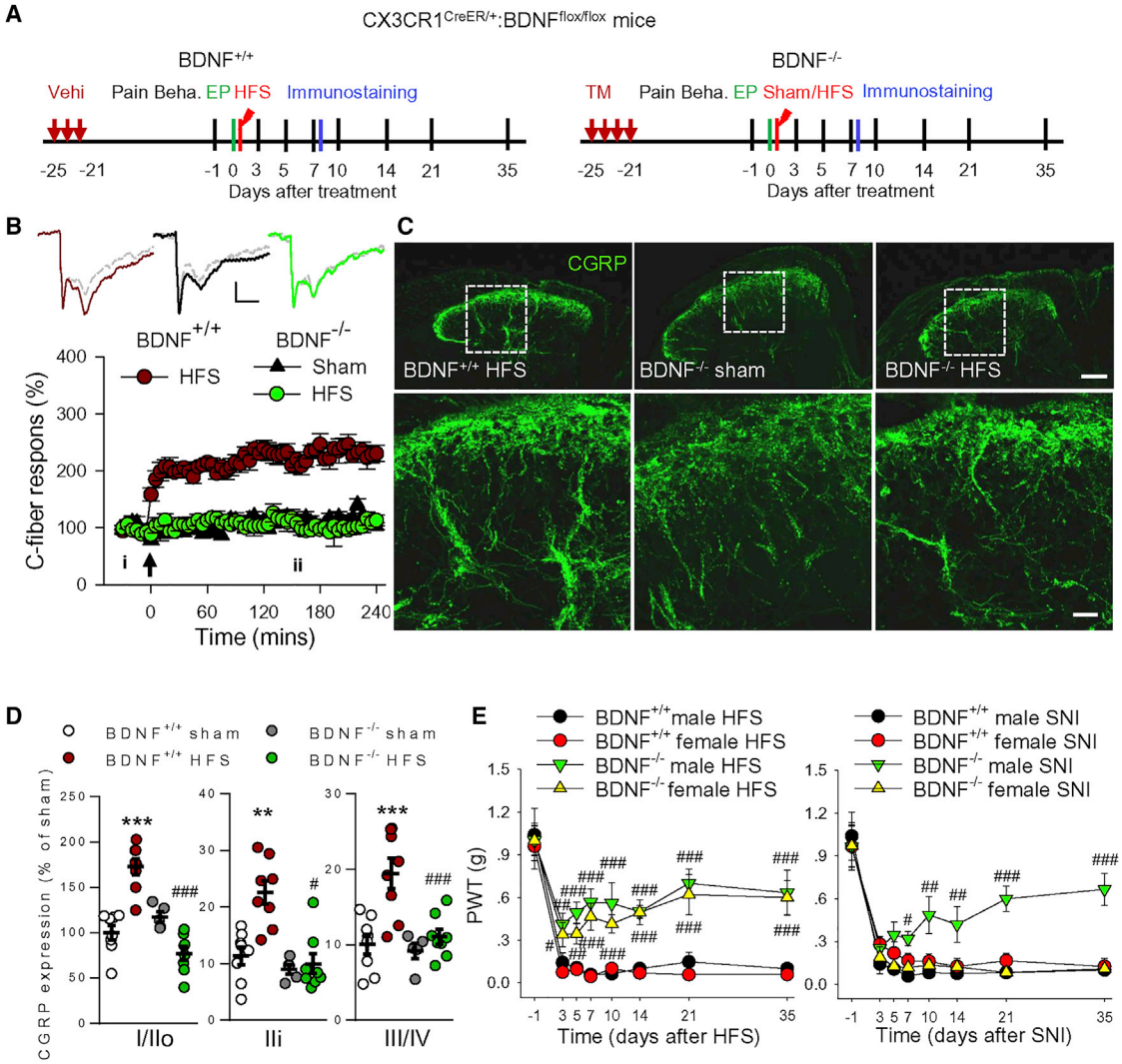

Figure 4. Ablation of Microglial BDNF Prevented LTP Induction, the Increase in CGRP Terminals, and Mechanical Allodynia Induced by HFS

(A) Schematic overview of experiments with BDNF$^{-/-}$, CX3CR1$^{CreER/+}$:BDNF$^{flox/flox}$ mice, in which BDNF can be specifically deleted from microglia by TM injection.

(B) 10V HFS induced spinal LTP in BDNF$^{+/+}$ mice but not in mice with microglial BDNF deletion (BDNF$^{-/-}$). n = 6–7 mice/group. Examples of C-fiber field potentials are shown above (i, gray lines) and 3 h after 10 V HFS (ii, color lines). Scale bars, 100 ms (x) and 0.2 mV (y). The arrow indicates the time point when conditional stimulation was delivered.

(C and D) Representative images (C) and summary data (D) showing that HFS-induced CGRP upregulation was inhibited by microglial BDNF ablation (n = 3–4 mice/group, 3–4 sections/mouse). ***p < 0.001 versus the BDNF$^{+/+}$ sham group, $^{###}$p < 0.001 versus the BDNF$^{+/+}$ HFS group; one-way ANOVA with Fisher's LSD test. Scale bars, 100 μm (top) and 20 μm (bottom).

(E) Unlike in the SNI model, HFS-induced mechanical allodynia was significantly reversed in male and female mice deficient of microglial BDNF compared with control mice. ***p < 0.001 versus the female BDNF$^{+/+}$ HFS or SNI group, two-way ANOVA with Fisher's LSD test.

CSF1 Signaling in Microglial Activation, LTP Induction, and Chronic Pain

It is unclear how HFS could activate spinal microglia in the sciatic nerve. A recent study showed that peripheral nerve injury induces *de novo* expression of CSF1 in injured DRG neurons. CSF1 activates microglia by binding to CSF1 receptors (CSF1Rs) that are exclusively expressed in microglia in the SDH (Guan et al., 2016). Therefore, we tested whether CSF1 signaling might also participate in 10 V HFS-induced microglial activation, spinal LTP, and chronic pain. To do this, we first examined the expression of CSF1 in DRGs and the dorsal horn after HFS. In DRG neurons, we found that CSF1 was expressed at a very low level in sham mice and upregulated gradually from 1 day to 7 days after 10 V HFS (Figures 5A and 5B). CSF1 expression induced by HFS was lower than that induced by SNI (Figure 5B). In SNI rats, CSF1 was expressed not only in injured DRG neurons (Figure 5A, ATF3^{+}, arrowheads) but also in uninjured neurons (ATF3^{-}, arrows), which is consistent with previous work (Guan et al., 2016). Interestingly, we found that, in the SDH, CSF1 was only co-localized with CGRP but not with IB4 (Figure 5C). These results

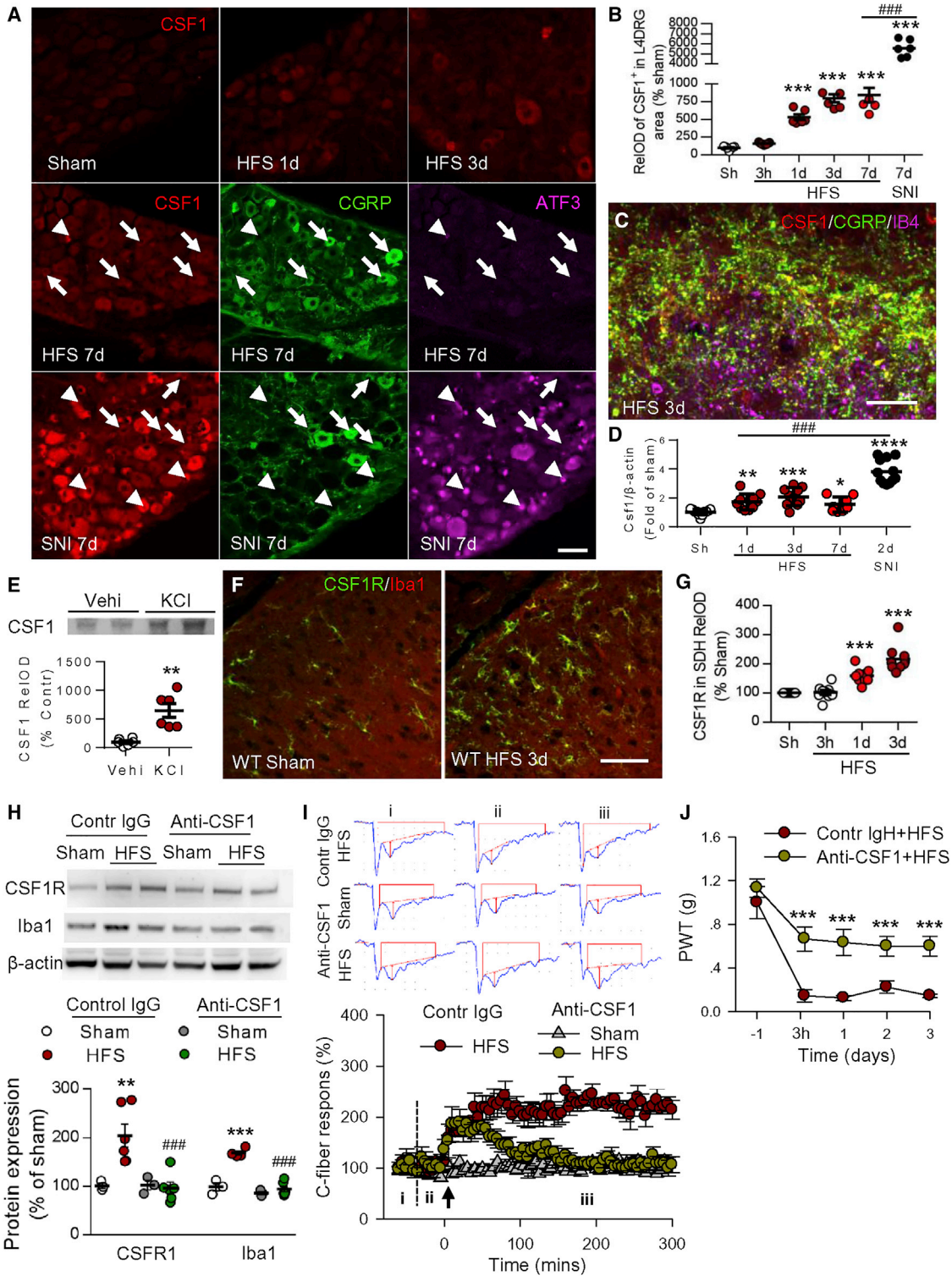

Figure 5. HFS Upregulates CSF1 in CGRP Terminals and CSF1 Receptors in Microglia, Leading to Spinal LTP and Pain Hypersensitivity

(A and B) Representative images (A) and statistical analysis (B) showing the expression of CSF1 in the ipsilateral L4 DRG from 1 to 7 days after HFS and 7 days after SNI. The triple staining images show colocalization of CSF1, CGRP, and ATF3. The arrowheads indicate that injured DRG neurons ($ATF3^{+}$) that strongly express CSF1 do not express CGRP. The arrows indicate uninjured neurons ($ATF3^{-}$) that weakly express CSF1 express CGRP following HFS or SNI. Scale bar, 50 μm. n = 3 mice/group, n = 2–3 images/mouse; *$p < 0.05$, ***$p < 0.001$ versus the sham group; $^{###}p < 0.001$ compared with the HFS 7-day group; one-way ANOVA with Tukey's post hoc test.

(legend continued on next page)

indicate that HFS upregulates CSF1 in DRG neurons and in CGRP$^+$ terminals in the SDH. Similarly, CSF1 mRNA progressively increased in ipsilateral L4–L5 DRGs from 1 day to 7 days after HFS (Figure 5D). Compared with HFS, SNI resulted in more significant enhancement in CSF1 mRNA 2 days after nerve injury. Moreover, in cultured DRG neurons, 40 mM KCl, which causes dramatic DRG neuron depolarization, significantly increased CSF1 in culture medium (Figure 5E), indicating that DRG neurons release CSF1 upon activation. Furthermore, immunofluorescence showed that HFS also significantly upregulated CSF1R in Iba1$^+$ microglia from 1 to 3 days after HFS (Figures 5F and 5G). Western blots revealed that both CSF1R and Iba1 were upregulated by HFS and that the changes were prevented by a single intrathecal injection of anti-CSF1 (40 ng/μL, 5 μl) 30 min before HFS (Figure 5H). This result indicates that CSF1 signaling is necessary for HFS-induced microglial activation. To determine the role of CSF1 signaling in spinal LTP, anti-CSF1 (40 ng/μL, 20 μL) was applied to the dorsal surface of the spinal cord 30 min before HFS. We found that anti-CSF1 did not affect basal transmission but blocked late-phase spinal LTP. Specifically, HFS-induced potentiation only lasted for approximately 1 h and then gradually returned to baseline, whereas application of immunoglobulin G (IgG) affected neither basal transmission nor LTP induction (Figure 5I). Consistently, we found a single intrathecal injection of CSF1 (6 ng/μL, 5 μL, daily for 3 days) induces mechanical allodynia lasting for around a week (Figure S7A) and upregulates CSF1R in activated spinal microglia (Figures S7B–S7E). This indicates that CSF1 is also sufficient to activate spinal microglia. Additionally, we found that the single intrathecal anti-CSF1 injection also substantially attenuated HFS-induced chronic allodynia (Figure 5J). These results suggest that HFS-induced CSF1 upregulation in DRGs and CGRP-afferent terminals is important for chronic pain.

CSF1 Signaling-Dependent Microglial BDNF in HFS-Induced Chronic Pain

We have demonstrated that both CSF1 signaling and microglial BDNF are required for HFS-induced functional and structural synaptic plasticity as well as pain hypersensitivity. However, it is still unknown whether CSF1 signaling and microglial BDNF are independently engaged in HFS-induced chronic pain. To determine whether there is a relationship between increased CSF1 signaling and upregulation of BDNF and CGRP, we applied anti-CSF1 antibody (40 ng/μL, 5 μL) intrathecally 30 min before HFS. We then examined BDNF and CGRP expression 3 days later. We found that anti-CSF1 treatment reduced both BDNF and CGRP upregulation otherwise induced by HFS (Figure 6A). To verify the effects of CSF1 on microglial activation and to investigate the underlying mechanisms, we performed experiments with cultured spinal cord slices. Treatment with CSF1 (1 μg/mL) for 6 h markedly upregulated microglial markers (CD11b and Iba1) as well as CSF1R expression. These effects were dose-dependently suppressed by the selective p38 mitogen-activated protein kinase (MAPK) inhibitor SB203580 (1 μM or 10 μM, added 1 h prior to CSF1) (Figures 6B–6D). Western blots showed that CSF1 application upregulated CSF1R, *p*-p38 MAPK, and BDNF. These increases were significantly blocked by SB203580 (Figure 6E). CSF1 also increased BDNF in culture medium, which could also be attenuated by SB203580 (Figure 6F). Because p38 is exclusively expressed in microglia in the SDH and its activation is critical for microglial activation (Ji and Suter, 2007), these *in vitro* experiments indicate that CSF1 is sufficient for microglial activation and BDNF release, whereas BDNF release depends on microglial activation.

Based on the above results, we hypothesized that activation of CSF1 signaling by HFS leads to microglial activation and that subsequent microglial BDNF release is critical for the increase in CGRP terminals and associated chronic pain behaviors. To directly test this hypothesis, we examined the effect of CSF1 on CGRP expression in the presence or absence of microglial BDNF. We found that intrathecal injection of CSF1 (20 ng/μL, 5 μL) increased CGRP expression only in control mice (BDNF$^{+/+}$) but not in CX3CR1$^{CreER/+}$:BDNF$^{flox/flox}$ mice 21 days after TM injection (BDNF$^{-/-}$), when BDNF was selectively deleted in microglia (Figure 6G). CSF1-induced mechanical allodynia was largely attenuated in mice deficient of microglial BDNF compared with control mice (Figure 6H). Therefore, microglial-specific BDNF is required for CSF1-induced CGRP upregulation and chronic pain.

DISCUSSION

LTP in the hippocampus is considered a biological substrate for some forms of memory (Bliss and Collingridge, 1993). To

(C) Triple staining showing that CSF1 in SDH was co-localized with CGRP but not with IB4 3 days after HFS. Scale bar, 20 μm.

(D) qRT-PCR analysis of CSF1 mRNA in ipsilateral L4–L5 DRGs from different groups (n = 7–12 mice/group). Values are presented as means ± SEM. *p < 0.05, **p < 0.01, ****p < 0.00001 versus the sham group; ###p < 0.001 compared with the HFS 7-day group; one-way ANOVA with Fisher's LSD test.

(E) Western blot and statistical analysis showing that treatment of cultured DRG neurons with 40 mM KCl for 24 h increased CSF1 in culture medium. n = 6 samples/group, **p < 0.01 versus Vehi group, unpaired Student's t test.

(F and G) Representative images (F) and statistical analysis (G) showing that CSF1R in microglia was upregulated in the ipsilateral dorsal horn 1 and 3 days after HFS (n = 3 mice/group, 2–3 sections/mouse). Scale bar, 50 μm. ***p < 0.001 compared with the sham group, ###p < 0.001 compared with the HFS 7-day group; one-way ANOVA with Tukey's post hoc test.

(H) Western blots illustrating the increased expression of CSF1R and Iba1 protein levels 3 days after 10 V HFS and that the changes were blocked by intrathecal injection of CSF1-neutralizing antibody (anti-CSF1, 40 ng/μL, 5 μL) 30 min before HFS (n = 3–4 mice/group). **p < 0.01, ***p < 0.001 versus the sham group; ###p < 0.001 versus the control HFS group; one-way ANOVA with Fisher's LSD test.

(I) Local application of anti-CSF1 (40 ng/μL, 20 μL) onto the dorsal surface of the spinal cord at recording segments 30 min before HFS did not affect the baseline of C-fiber responses but blocked the late phase of the spinal LTP (n = 5–6 mice/group). Original traces of C-fiber fEPSPs from different groups, recorded at baseline (i), 30 min before (ii), and 3 h (iii) after HFS, are shown at the top. Scale bars, 100 ms (x) and 0.2 mV (y). The arrow indicates the time point when conditional stimulation was delivered.

(J) Intrathecal injection of anti-CSF1 antibody 30 min before HFS prevented the development of mechanical hypersensitivity (n = 6 mice/group, ***p < 0.001 versus the Vehi group, two-way ANOVA with Fisher's LSD test).

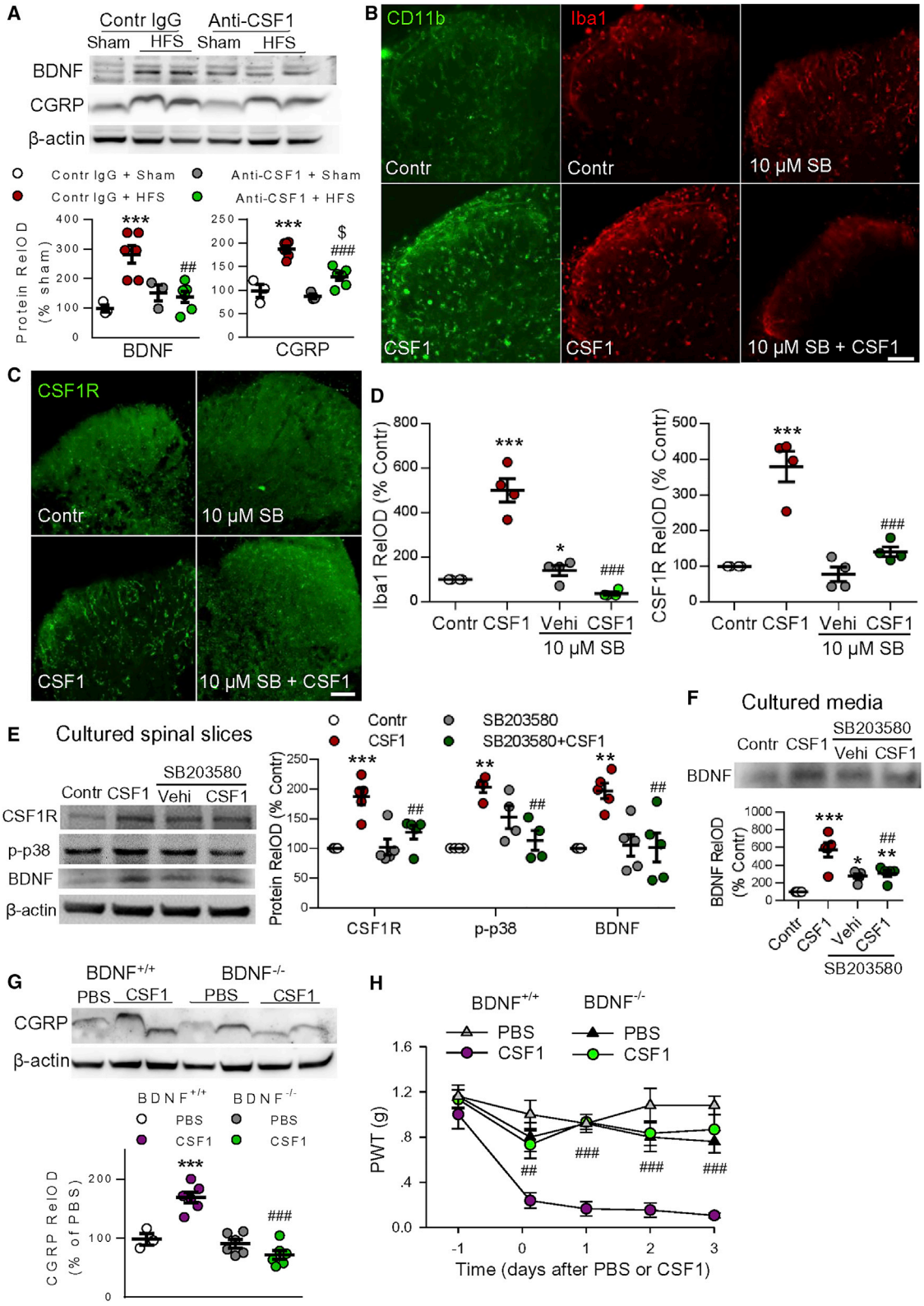

(legend on next page)

date, however, a definitive demonstration indicating that memory and LTP share the same cellular and molecular mechanisms and that induction of LTP will result in some form of memory is still lacking (Lynch, 2004). This is difficult to achieve, largely because of the complexity in synaptic connections and functions of the hippocampus. On the other hand, spinal LTP at C-fiber (pain fiber) synapses (Liu and Sandkühler, 1995) is believed to be a pain memory that may underlie some forms of chronic pain (Liu and Zhou, 2015). The present work provides evidence supporting the hypothesis that induction of LTP at synapses between afferent C-fibers and dorsal horn neurons by 10 V HFS is associated with mechanical allodynia lasting for 50 days in rats (Figure S2B) and more than 35 days in mice (Figure 4E) as well as thermal hyperalgesia for around 14 days (Figure 1H). A microglial BDNF-dependent increase in (or sprouting of) CGRP terminals, which is found in a variety of chronic pain conditions (Christensen and Hulsebosch, 1997; Xu et al., 2017; Zheng et al., 2008), serves as a structural basis of the chronic pain. Our finding is also clinically important because chronic pain, unlike acute pain, rarely has an identifiable temporal and causal relationship with injury or disease in the body. Chronic pain with unknown etiology was recently classified as chronic primary pain (Treede et al., 2015), with the underlying mechanism still poorly understood. Spinal LTP at C-fiber synapses can be induced in many ways, including peripheral nerve injury (Zhang et al., 2004), activation of presynaptic terminals by electrical stimulation of afferent C-fibers (Liu and Sandkühler, 1995), or direct activation of glial cells by local application of BDNF (Zhou et al., 2008), fractalkine (Clark et al., 2015) or ATP receptor agonists (Kronschläger et al., 2016) without direct activation of the presynaptic component. At present, it is generally believed that chronic pain is produced by nerve injury (neuropathic pain) and/or inflammation (inflammatory pain) (Yekkirala et al., 2017). Here we show that HFS-induced chronic pain in naive mice is neither associated with nerve injury nor inflammation near the stimulated nerve (Figures 1B–1F). Therefore, we exposed a form of chronic pain that is produced by activation of spinal microglia through intensive peripheral nerve stimuli (Figure 7). This mechanism may be an important insight into explaining chronic pain without a clinically obvious cause.

Action Potential Discharge in Nociceptive Afferents Evoked by HFS Underlie Chronic Pain

Sturge (1883) demonstrated that peripheral injury triggers a change in CNS excitability so that normal inputs evoke exaggerated responses as part of pain hypersensitivity. Consistent with this notion, nerve injury has been shown to induce a transient action potential discharge in afferent A- and C-fibers within the first seconds following injury (Liu et al., 2000). This phenomenon, called injury discharge, is believed to trigger chronic pain. To date, however, whether the injury discharge alone is sufficient to generate chronic pain is still unknown because peripheral nerve injury also causes hypersensitivity of the afferent neurons.

Our previous work shows that injury of the sciatic nerve induces LTP at C-fiber synapses within minutes and that the effect is completely prevented by blocking action potential conduction with lidocaine (Zhang et al., 2004), indicating that the injury discharge is sufficient to induce spinal LTP. In the current study, we showed that HFS at the sciatic nerve triggered long-lasting pain hypersensitivity in mice by inducing spinal LTP without any observable nerve injury. Temporally, HFS induced spinal LTP within a few minutes and pain hypersensitivity in about 30 min. Inhibition of LTP by local application of lidocaine to the sciatic nerve or by intrathecal injection of an NMDA receptor antagonist prevented chronic pain (Figures 1I and 1J; Figure S1). However, HFS at A-fibers neither induced LTP nor chronic pain. Activation of spinal NMDA receptors through HFS of nociceptive afferents is sufficient to induce chronic pain hypersensitivity. These effects are not associated with any other changes in the periphery that might be produced by HFS. Interestingly, we have shown that action potential discharges in primary afferent C-fibers by HFS are sufficient to activate spinal microglia. Consequently, HFS may potentially induce neurogenic neuroinflammation in the spinal cord as the root cause of chronic pain.

The Roles of Peptidergic C-fiber Terminals in Initiation and Maintenance of HFS-Induced Chronic Pain Hypersensitivity

Peptidergic C-fiber terminals express and release bioactive substances, including glutamate, CGRP, SP, BDNF (Lever et al., 2001), ATP (Kronschläger et al., 2016), fractalkine (Clark et al., 2015), and CASP6 (Berta et al., 2014). These released signaling molecules play a role in spinal LTP and pain hypersensitivity by

Figure 6. Microglial BDNF Is Required for an CSF1-Induced Increase in CGRP Terminals and Pain Hypersensitivity

(A) HFS upregulated BDNF and CGRP levels in the SDH, and the effects were prevented by intrathecal injection of anti-CSF1 (40.0 ng/μL) 30 min before HFS (n = 3–6 mice/group). ***p < 0.001 versus the control sham group; ##p < 0.01, ###p < 0.001 versus the control HFS group; $p < 0.05 versus the anti-CSF1 sham group; one-way ANOVA with Fisher's LSD test.

(B and C) In cultured spinal cord slices, CSF1 (1 μg/mL) markedly upregulated microglial markers (CD11b and Iba1, B) and CSF1R (C), and the effects were dose-dependently suppressed by the p38 MAPK inhibitor SB203580 (10 μM) applied 1 h prior to CSF1. Scale bar, 100 μm.

(D) Pooled results showing the difference in Iba1 or CSF1R expression in different groups. n = 4–5 samples/group; *p < 0.05, ***p < 0.001 versus the control group; ###p < 0.001 versus the CSF1 group; one-way ANOVA with Tukey's post hoc test.

(E and F) In culture spinal cord slices, treatment with CSF1 for 6 h upregulated CSF1R, phospho-p38 MAPK (*p*-p38), and BDNF (E) as well as increased BDNF in culture medium (F). Pretreatment with the p38 inhibitor SB203580 (10 μM) abolished the effects of CSF1. n = 3–5 samples/group; **p < 0.01, ***p < 0.001 versus the control group; ##p < 0.01 versus the CSF1 group; one-way ANOVA with Tukey's post hoc test.

(G) Intrathecal CSF1 upregulated CGRP expression in $BDNF^{+/+}$ mice but not in mice deficient of microglial BDNF ($BDNF^{-/-}$), as measured 3 days after injection (n = 3–6 mice/group). ***p < 0.001 versus the $BDNF^{+/+}$PBS group, ###p < 0.001 versus the $BDNF^{+/+}$ CSF1 group; one-way ANOVA with Fisher's LSD test.

(H) Mechanical allodynia induced by intrathecal CSF1 was significantly attenuated in microglial BDNF deletion mice compared with control mice (n = 5–6 mice/group, ###p < 0.001 versus the $BDNF^{+/+}$ CSF1 group, two-way ANOVA with Fisher's LSD test).

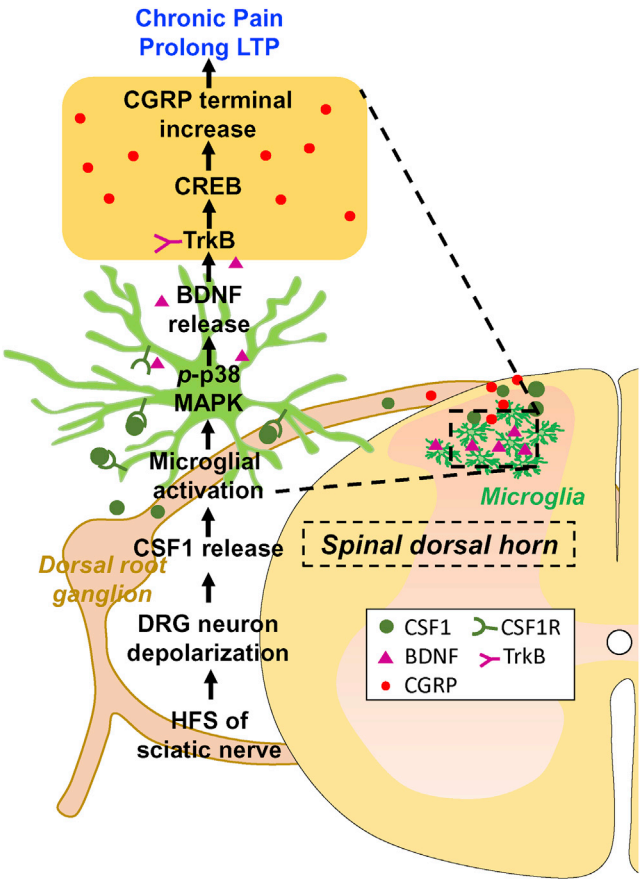

Figure 7. The Mechanism of HFS of Sciatic Nerve-Induced Chronic Pain without Stimulated Sciatic Nerve Injury

HFS of the sciatic nerve depolarizes DRG neurons to release CSF1 from the central terminals. CSF1 activates microglial CSF1R/p38 MAPK to release BDNF. BDNF causes an increase in CGRP terminals via TrkB/CREB signaling. Microglia activation and the CGRP terminal increase underlie prolonged LTP and chronic pain.

volume transmission as well as by classical synaptic transmission (Borroto-Escuela et al., 2015). For example, both NK1 and NK2 SP receptors are required for spinal LTP induction (Liu and Sandkühler, 1997). Spinal application of BDNF directly induces late-phase spinal LTP and mechanical allodynia by activation of microglia (Zhou et al., 2011). Human studies suggest that activation of peptidergic cutaneous afferents is responsible for HFS-induced mechanical allodynia (Pfau et al., 2011). Together, activation of peptidergic C-fibers is critical for induction of spinal LTP at C-fiber synapses.

CGRP has been identified as an important molecule in spinal nociceptive processing and in migraine headache (Edvinsson et al., 2018). Increases in CGRP afferents in SDH has been reported in a variety of chronic pain conditions, such as vincristine-induced neuropathy (Xu et al., 2017), sciatic nerve crush or transection (Zheng et al., 2008), and spinal cord hemisection (Christensen and Hulsebosch, 1997). In the present work, we showed that CGRP terminals, the number of $CGRP^+$ varicosities, and the number of $CGRP^+$ synapses increased significantly in the dorsal horn following HFS (Figures 2C–2F). Importantly, in $CGRP^+$ terminals, synaptophysin, SP, and GAP43 were significantly increased after HFS (Figure S4). These data suggest that the increase in $CGRP^+$ terminals results from axon sprouting. Therefore, we presumed that the increase in CGRP terminals may be critical for the transition from acute pain to chronic pain.

NMDA receptors are critical for the induction of spinal LTP (Liu and Sandkühler, 1995). In the present work, we demonstrated that blocking NMDA receptors with D-AP5 suppressed HFS-induced CGRP increases (Figures 2G and 2H), which is consistent with previous studies (Csáti et al., 2015; Wong et al., 2014). Because synaptic functional plasticity leads to structural plasticity, the effect of the NMDA receptor antagonist D-AP5 on CGRP terminals may result from inhibition of spinal LTP. Because NMDA receptors are also expressed in the presynaptic terminal and facilitate glutamate release from primary afferents (Chen et al., 2014; Liu et al., 1994), it is also possible that the activation of NMDA receptors directly upregulates CGRP expression and release in the dorsal horn. Further studies are needed to clarify this issue.

The Roles of Microglia and BDNF in HFS-Induced LTP and Chronic Pain

Previous work shows that activation of microglia by fractalkine (CX3CL1), ATP, interleukin-1β (IL-1β), and tumor necrosis factor alpha (TNF-α) is critical for the induction of spinal LTP (Clark et al., 2015; Gruber-Schoffnegger et al., 2013; Wang et al., 2018). In the present study, we further tested the role of microglia in spinal LTP by depleting resident microglia but not peripheral monocytes or macrophages using $CX3CR1^{CreER/+}$:$R26^{iDTR/+}$ transgenic mice. Our results showed that selective deletion of spinal microglia blocked HFS-induced LTP, the increase in $CGRP^+$ terminals, and chronic pain hypersensitivity (Figure 3).

How can HFS activate spinal microglia? A previous study shows that electrical stimuli (5 Hz, 0.5 ms, 0.1–10 mA, a total of 3,000 pulses for 10 min) activate spinal glial cell and also induce nerve degeneration in rats (Shortland et al., 1997). Our previous study demonstrated that 400 pulses of electrical stimulation at 2 Hz, 20 Hz, or 100 Hz at 30–40 V but not 3 V could induce spinal LTP in rats (Liu and Sandkühler, 1997). In the present study, we found that 400-pulse HFS at 10 V (100 Hz, 0.5 ms, 4 trains of 1-s duration at 10-s intervals) was an effective electrical stimulation paradigm in mice for LTP that also leads to spinal microglia activation and long-lasting mechanical hypersensitivity without stimulated nerve injury. Collectively, different electrical stimulating parameters (such as intensity, frequency, and duration) have different influences on microglial activation. In addition, previous studies showed that microglial activation induced by electrical stimulation of the sciatic nerve at C-fiber intensities can be blocked by the NK1 receptor antagonist LY303870 (Li et al., 2015). Direct activation of glial cells by local application of BDNF (Zhou et al., 2011), CASP6 (Berta et al., 2014), fractalkine (Clark et al., 2015), TNF, or ATP receptor agonists (Kronschläger et al., 2016) is sufficient to induce spinal LTP and pain hypersensitivity through microglia without causing axonal degeneration. Therefore, spinal microglia are able to sense nociceptive signals, and the neuromodulators (such as SP, ATP,

BDNF, CASP6, or CSF1) released from peptidergic C-fibers are essential for rapid microglial activation.

Previous work (Guan et al., 2016) showed that CSF1 is upregulated in injured DRG neurons 1 day but not 12 h after peripheral nerve injury. CSF1Rs, which are exclusively expressed in microglia in the SDH, are upregulated 2–3 days after nerve injury. CSF1 in injured DRG neurons is suggested to transport to the SDH, where it activates microglia by binding to CSF1Rs. In the present work, we found that 10 V HFS also upregulated CSF1 mRNA and protein in DRG neurons, although the magnitude of the upregulation was weaker than that induced by SNI (Figures 5A, 5B, and 5D). Importantly, HFS upregulates CSF1 only in $CGRP^+$ terminals in the SDH (Figure 5C). HFS also upregulated CSF1R in spinal microglia. Our results showed that HFS-induced LTP and pain hypersensitivity occurred swiftly (within hours), whereas CGRP was upregulated days after HFS (Figure 2). These results suggest that HFS-induced LTP might be the trigger for later biochemical changes in the SDH. In terms of Iba1 upregulation 3 days after HFS (Figure 3), this may reflect late activation of microglia. HFS may acutely activate microglia through CSF1 signaling within hours, when Iba1 upregulation did not yet happen. We propose that spinal microglia are activated by neurotransmitters released from $CGRP^+$ C-termini immediately after HFS and later by CSF1, which is increased in $CGRP^+$ terminals. Therefore, $CGRP^+$ C-termini are critically involved in the initiation and maintenance of microglial activation in SDH.

It is well established that activation of the BDNF/TrkB pathway is essential for both spinal LTP induction (Zhou et al., 2008) and the development of neuropathic pain (Coull et al., 2005). BDNF expressed in peptidergic DRG neurons is released from central terminals in the SDH in response to short bursts of HFS at C-fiber strength (300 pulses in 75 trains, 100 Hz) along with SP and glutamate (Lever et al., 2001). Selective deletion of BDNF in nociceptive DRG neurons impairs the inflammatory pain induced by formalin or carrageenan injection; however, it does not affect neuropathic pain (Zhao et al., 2006). Consistent with previous work (Sorge et al., 2015), we found that genetic depletion of BDNF from microglia attenuates nerve injury-induced mechanical allodynia in male but not in female mice (Figure 4E). However, microglial BDNF deletion prevents HFS-induced LTP, CGRP upregulation, and mechanical allodynia in both male and female mice (Figure 4E). Our data confirmed that BDNF was sufficient to enhance $CGRP^+$ terminals *in vivo* and *in vitro*. Previous work showed TrkB expression in CGRP peptidergic C-fiber terminals (Merighi et al., 2008). We further uncovered that the BDNF/TrkB/CREB signaling pathway is involved in CGRP terminal increase.

Although our results indicate an important role of microglial BDNF in chronic pain induced by nerve injury and HFS, recent studies show that BDNF gene expression is at very low levels in microglia of the adult brain (Bennett et al., 2016) and spinal cord (Denk et al., 2016). Therefore, BDNF released from microglia might be limited. How the small amount of BDNF is so important for chronic pain remains elusive. In addition, it is still unknown how BDNF from diverse sources (nociceptive afferents versus microglia) differentially affects inflammatory pain and neuropathic pain and why deletion of microglial BDNF attenuates neuropathic pain only in male mice but suppresses HFS-induced chronic pain in both male and female mice. We believe that the discrepancy could be due to the different pain models; i.e., HFS-induced chronic pain versus nerve injury-induced neuropathic pain. Further studies are needed to clarify these issues. Interestingly, our previous study showed that inhibition of BDNF signaling did not affect LTP induced by 40 V HFS in rats (Zhou et al., 2008). The discrepancy could be due to the potential damage to the stimulated nerve by 40 V HFS, as reported previously (Liang et al., 2010). Therefore, both nerve injury and activation of afferent fibers contribute to HFS-induced LTP, likely using different signaling pathways.

In summary, we report that the electrical HFS that induces spinal LTP at C-fiber synapses without causing injury of the stimulated nerve leads to long-lasting mechanical allodynia and thermal hyperalgesia in mice. Our findings may explain chronic primary pain that occurs in the absence of injury or disease.

STAR★METHODS

Detailed methods are provided in the online version of this paper and include the following:

- KEY RESOURCES TABLE
- CONTACT FOR REAGENT AND RESOURCE SHARING
- EXPERIMENTAL MODEL AND SUBJECT DETAILS
  - Animals and husbandry
  - Electrical stimulation-induced chronic pain model
  - Spared nerve injury
- METHOD DETAILS
  - Microglia ablation and repopulation
  - Microglial BDNF deletion
  - *In vivo* extracellular recordings in the dorsal horn
  - Behavioral tests
  - Local application of lidocaine around the sciatic nerve
  - Intrathecal injection of drugs
  - Fluorescent immunohistochemical staining
  - Western blot
  - Ultrastructure of rat sciatic nerves
  - Pre-embedding immunoelectron microscopy (IEM)
  - qRT-PCR
  - Culture of DRG neurons
  - Acute spinal cord slice culture
- QUANTIFICATION AND STATISTICAL ANALYSIS
  - Statistical analysis
  - Quantification of immunofluorescence staining
  - TEM analysis
  - IEM analysis
  - Analysis of CGRP neurite length

SUPPLEMENTAL INFORMATION

Supplemental Information can be found online at https://doi.org/10.1016/j.celrep.2019.05.087.

ACKNOWLEDGMENTS

This work was supported by the National Institutes of Health, United States (R21DE025689 and R01NS088627), the National Natural Science Foundation of China (81771204, U1201223, 8137119, and 81270377), the Guangdong Province University Outstanding Young Teachers' Training Program (Yq2013008),

and the Natural Science Foundation of Guangdong Province, China (S2013010011889 and 2014A030313062). We thank Dr. Wen-Biao Gan (New York University) for providing CX3CR1$^{CreER/+}$ mice and Noriko Goldsmith (Rutgers University) for technical assistance with confocal microscopy. Also, we greatly appreciate all members of the Wu lab at Rutgers University and the Mayo Clinic for insightful discussions.

AUTHOR CONTRIBUTIONS

L.-J.Z., J.R.R., Z.T., X.-G.L., and L.-J.W. conceived the study, designed the experiments, and wrote the manuscript. L.-J.Z. performed most of the experiments. J.P. and Y.-N.X. performed intrathecal injection of drugs and performed all blind pain behavior tests. L.-J.Z., Y.-N.X., W.-J.Z., and J.Z. performed the spinal culture, DRG neuron culture, and qRT-PCR experiments. W.-J.Z., Z.T., and T.C. performed the IEM experiments and data analysis. X.W. performed the experiment in rats. C.-L.M., Z.-J.L., Y.L., M.M., U.B.E., A.D.U., W.-J.X., M.L., and H.W. assisted with experiments.

DECLARATION OF INTERESTS

The authors declare no competing interests.

Received: April 19, 2018
Revised: January 29, 2019
Accepted: May 22, 2019
Published: June 25, 2019

REFERENCES

Bangratz, M., Sarrazin, N., Devaux, J., Zambroni, D., Echaniz-Laguna, A., René, F., Boërio, D., Davoine, C.S., Fontaine, B., Feltri, M.L., et al. (2012). A mouse model of Schwartz-Jampel syndrome reveals myelinating Schwann cell dysfunction with persistent axonal depolarization in vitro and distal peripheral nerve hyperexcitability when perlecan is lacking. Am. J. Pathol. *180*, 2040–2055.

Bennett, M.L., Bennett, F.C., Liddelow, S.A., Ajami, B., Zamanian, J.L., Fernhoff, N.B., Mulinyawe, S.B., Bohlen, C.J., Adil, A., Tucker, A., et al. (2016). New tools for studying microglia in the mouse and human CNS. Proc. Natl. Acad. Sci. USA *113*, E1738–E1746.

Benowitz, L.I., and Routtenberg, A. (1997). GAP-43: an intrinsic determinant of neuronal development and plasticity. Trends Neurosci. *20*, 84–91.

Berta, T., Park, C.K., Xu, Z.Z., Xie, R.G., Liu, T., Lü, N., Liu, Y.C., and Ji, R.R. (2014). Extracellular caspase-6 drives murine inflammatory pain via microglial TNF-α secretion. J. Clin. Invest. *124*, 1173–1186.

Bliss, T.V., and Collingridge, G.L. (1993). A synaptic model of memory: long-term potentiation in the hippocampus. Nature *361*, 31–39.

Borroto-Escuela, D.O., Agnati, L.F., Bechter, K., Jansson, A., Tarakanov, A.O., and Fuxe, K. (2015). The role of transmitter diffusion and flow versus extracellular vesicles in volume transmission in the brain neural-glial networks. Philos. Trans. R. Soc. Lond. B Biol. Sci. *370*, 20140183.

Chen, S.R., Hu, Y.M., Chen, H., and Pan, H.L. (2014). Calcineurin inhibitor induces pain hypersensitivity by potentiating pre- and postsynaptic NMDA receptor activity in spinal cords. J. Physiol. *592*, 215–227.

Chen, L.H., Sun, Y.T., Chen, Y.F., Lee, M.Y., Chang, L.Y., Chang, J.Y., and Shen, M.R. (2015). Integrating Image-Based High-Content Screening with Mouse Models Identifies 5-Hydroxydecanoate as a Neuroprotective Drug for Paclitaxel-Induced Neuropathy. Mol. Cancer Ther. *14*, 2206–2214.

Christensen, M.D., and Hulsebosch, C.E. (1997). Spinal cord injury and anti-NGF treatment results in changes in CGRP density and distribution in the dorsal horn in the rat. Exp. Neurol. *147*, 463–475.

Clark, A.K., Gruber-Schoffnegger, D., Drdla-Schutting, R., Gerhold, K.J., Malcangio, M., and Sandkühler, J. (2015). Selective activation of microglia facilitates synaptic strength. J. Neurosci. *35*, 4552–4570.

Coull, J.A., Beggs, S., Boudreau, D., Boivin, D., Tsuda, M., Inoue, K., Gravel, C., Salter, M.W., and De Koninck, Y. (2005). BDNF from microglia causes the shift in neuronal anion gradient underlying neuropathic pain. Nature *438*, 1017–1021.

Csáti, A., Edvinsson, L., Vécsei, L., Toldi, J., Fülöp, F., Tajti, J., and Warfvinge, K. (2015). Kynurenic acid modulates experimentally induced inflammation in the trigeminal ganglion. J. Headache Pain *16*, 99.

Decosterd, I., and Woolf, C.J. (2000). Spared nerve injury: an animal model of persistent peripheral neuropathic pain. Pain *87*, 149–158.

Denk, F., Crow, M., Didangelos, A., Lopes, D.M., and McMahon, S.B. (2016). Persistent Alterations in Microglial Enhancers in a Model of Chronic Pain. Cell Rep. *15*, 1771–1781.

Edvinsson, L., Haanes, K.A., Warfvinge, K., and Krause, D.N. (2018). CGRP as the target of new migraine therapies - successful translation from bench to clinic. Nat. Rev. Neurol. *14*, 338–350.

Flatters, S.J., and Bennett, G.J. (2006). Studies of peripheral sensory nerves in paclitaxel-induced painful peripheral neuropathy: evidence for mitochondrial dysfunction. Pain *122*, 245–257.

Gruber-Schoffnegger, D., Drdla-Schutting, R., Hönigsperger, C., Wunderbaldinger, G., Gassner, M., and Sandkühler, J. (2013). Induction of thermal hyperalgesia and synaptic long-term potentiation in the spinal cord lamina I by TNF-α and IL-1β is mediated by glial cells. J. Neurosci. *33*, 6540–6551.

Gu, N., Peng, J., Murugan, M., Wang, X., Eyo, U.B., Sun, D., Ren, Y., DiCicco-Bloom, E., Young, W., Dong, H., and Wu, L.J. (2016). Spinal Microgliosis Due to Resident Microglial Proliferation Is Required for Pain Hypersensitivity after Peripheral Nerve Injury. Cell Rep. *16*, 605–614.

Guan, Z., Kuhn, J.A., Wang, X., Colquitt, B., Solorzano, C., Vaman, S., Guan, A.K., Evans-Reinsch, Z., Braz, J., Devor, M., et al. (2016). Injured sensory neuron-derived CSF1 induces microglial proliferation and DAP12-dependent pain. Nat. Neurosci. *19*, 94–101.

Hargreaves, K., Dubner, R., Brown, F., Flores, C., and Joris, J. (1988). A new and sensitive method for measuring thermal nociception in cutaneous hyperalgesia. Pain *32*, 77–88.

Inoue, K., and Tsuda, M. (2018). Microglia in neuropathic pain: cellular and molecular mechanisms and therapeutic potential. Nat. Rev. Neurosci. *19*, 138–152.

Ji, R.R., and Suter, M.R. (2007). p38 MAPK, microglial signaling, and neuropathic pain. Mol. Pain *3*, 33.

Jun, B.K., Chandra, A., Kuljis, D., Schmidt, B.P., and Eichler, F.S. (2015). Substrate Availability of Mutant SPT Alters Neuronal Branching and Growth Cone Dynamics in Dorsal Root Ganglia. J. Neurosci. *35*, 13713–13719.

Kronschläger, M.T., Drdla-Schutting, R., Gassner, M., Honsek, S.D., Teuchmann, H.L., and Sandkühler, J. (2016). Gliogenic LTP spreads widely in nociceptive pathways. Science *354*, 1144–1148.

Lever, I.J., Bradbury, E.J., Cunningham, J.R., Adelson, D.W., Jones, M.G., McMahon, S.B., Marvizón, J.C., and Malcangio, M. (2001). Brain-derived neurotrophic factor is released in the dorsal horn by distinctive patterns of afferent fiber stimulation. J. Neurosci. *21*, 4469–4477.

Li, W.W., Guo, T.Z., Shi, X., Sun, Y., Wei, T., Clark, D.J., and Kingery, W.S. (2015). Substance P spinal signaling induces glial activation and nociceptive sensitization after fracture. Neuroscience *310*, 73–90.

Liang, L., Wang, Z., Lü, N., Yang, J., Zhang, Y., and Zhao, Z. (2010). Involvement of nerve injury and activation of peripheral glial cells in tetanic sciatic stimulation-induced persistent pain in rats. J. Neurosci. Res. *88*, 2899–2910.

Liu, X.G., and Sandkühler, J. (1995). Long-term potentiation of C-fiber-evoked potentials in the rat spinal dorsal horn is prevented by spinal N-methyl-D-aspartic acid receptor blockage. Neurosci. Lett. *191*, 43–46.

Liu, X., and Sandkühler, J. (1997). Characterization of long-term potentiation of C-fiber-evoked potentials in spinal dorsal horn of adult rat: essential role of NK1 and NK2 receptors. J. Neurophysiol. *78*, 1973–1982.

Liu, X.G., and Zhou, L.J. (2015). Long-term potentiation at spinal C-fiber synapses: a target for pathological pain. Curr. Pharm. Des. *21*, 895–905.

Liu, H., Wang, H., Sheng, M., Jan, L.Y., Jan, Y.N., and Basbaum, A.I. (1994). Evidence for presynaptic N-methyl-D-aspartate autoreceptors in the spinal cord dorsal horn. Proc. Natl. Acad. Sci. USA *91*, 8383–8387.

Liu, X., Eschenfelder, S., Blenk, K.H., Jänig, W., and Häbler, H. (2000). Spontaneous activity of axotomized afferent neurons after L5 spinal nerve injury in rats. Pain *84*, 309–318.

Liu, Y., Zhou, L.J., Wang, J., Li, D., Ren, W.J., Peng, J., Wei, X., Xu, T., Xin, W.J., Pang, R.P., et al. (2017). TNF-α Differentially Regulates Synaptic Plasticity in the Hippocampus and Spinal Cord by Microglia-Dependent Mechanisms after Peripheral Nerve Injury. J. Neurosci. *37*, 871–881.

Lynch, M.A. (2004). Long-term potentiation and memory. Physiol. Rev. *84*, 87–136.

Matsuura, Y., Ohtori, S., Iwakura, N., Suzuki, T., Kuniyoshi, K., and Takahashi, K. (2013). Expression of activating transcription factor 3 (ATF3) in uninjured dorsal root ganglion neurons in a lower trunk avulsion pain model in rats. Eur. Spine J. *22*, 1794–1799.

Merighi, A., Bardoni, R., Salio, C., Lossi, L., Ferrini, F., Prandini, M., Zonta, M., Gustincich, S., and Carmignoto, G. (2008). Presynaptic functional trkB receptors mediate the release of excitatory neurotransmitters from primary afferent terminals in lamina II (substantia gelatinosa) of postnatal rat spinal cord. Dev. Neurobiol. *68*, 457–475.

Orita, S., Eguchi, Y., Kamoda, H., Arai, G., Ishikawa, T., Miyagi, M., Inoue, G., Suzuki, M., Toyone, T., Aoki, Y., et al. (2011). Brain-derived neurotrophic factor inhibition at the punctured intervertebral disc downregulates the production of calcitonin gene-related peptide in dorsal root ganglia in rats. Spine *36*, 1737–1743.

Parkhurst, C.N., Yang, G., Ninan, I., Savas, J.N., Yates, J.R., 3rd, Lafaille, J.J., Hempstead, B.L., Littman, D.R., and Gan, W.B. (2013). Microglia promote learning-dependent synapse formation through brain-derived neurotrophic factor. Cell *155*, 1596–1609.

Peng, J., Gu, N., Zhou, L., B Eyo, U., Murugan, M., Gan, W.B., and Wu, L.J. (2016). Microglia and monocytes synergistically promote the transition from acute to chronic pain after nerve injury. Nat. Commun. *7*, 12029.

Pfau, D.B., Klein, T., Putzer, D., Pogatzki-Zahn, E.M., Treede, R.D., and Magerl, W. (2011). Analysis of hyperalgesia time courses in humans after painful electrical high-frequency stimulation identifies a possible transition from early to late LTP-like pain plasticity. Pain *152*, 1532–1539.

Saeed, A.W., and Ribeiro-da-Silva, A. (2012). Non-peptidergic primary afferents are presynaptic to neurokinin-1 receptor immunoreactive lamina I projection neurons in rat spinal cord. Mol. Pain *8*, 64.

Sandkühler, J., and Gruber-Schoffnegger, D. (2012). Hyperalgesia by synaptic long-term potentiation (LTP): an update. Curr. Opin. Pharmacol. *12*, 18–27.

Seltzer, Z., Cohn, S., Ginzburg, R., and Beilin, B. (1991). Modulation of neuropathic pain behavior in rats by spinal disinhibition and NMDA receptor blockade of injury discharge. Pain *45*, 69–75.

Shortland, P., Kinman, E., and Molander, C. (1997). Sprouting of A-fibre primary afferents into lamina II in two rat models of neuropathic pain. Eur. J. Pain *1*, 215–227.

Song, X.Y., Li, F., Zhang, F.H., Zhong, J.H., and Zhou, X.F. (2008). Peripherally-derived BDNF promotes regeneration of ascending sensory neurons after spinal cord injury. PLoS ONE *3*, e1707.

Sorge, R.E., Mapplebeck, J.C., Rosen, S., Beggs, S., Taves, S., Alexander, J.K., Martin, L.J., Austin, J.S., Sotocinal, S.G., Chen, D., et al. (2015). Different immune cells mediate mechanical pain hypersensitivity in male and female mice. Nat. Neurosci. *18*, 1081–1083.

Sturge, W.A. (1883). The Phenomen of Angina Pectoris, and Their Bearing Upon The theory of Counter-Irritation. Brain *5*, 492–510.

Treede, R.D., Rief, W., Barke, A., Aziz, Q., Bennett, M.I., Benoliel, R., Cohen, M., Evers, S., Finnerup, N.B., First, M.B., et al. (2015). A classification of chronic pain for ICD-11. Pain *156*, 1003–1007.

Wang, Z.C., Li, L.H., Bian, C., Yang, L., Lv, N., and Zhang, Y.Q. (2018). Involvement of NF-κB and the CX3CR1 signaling network in mechanical allodynia induced by tetanic sciatic stimulation. Neurosci. Bull. *34*, 64–73.

Wong, H., Kang, I., Dong, X.D., Christidis, N., Ernberg, M., Svensson, P., and Cairns, B.E. (2014). NGF-induced mechanical sensitization of the masseter muscle is mediated through peripheral NMDA receptors. Neuroscience *269*, 232–244.

Xu, T., Li, D., Zhou, X., Ouyang, H.D., Zhou, L.J., Zhou, H., Zhang, H.M., Wei, X.H., Liu, G., and Liu, X.G. (2017). Oral Application of Magnesium-L-Threonate Attenuates Vincristine-induced Allodynia and Hyperalgesia by Normalization of Tumor Necrosis Factor-α/Nuclear Factor-κB Signaling. Anesthesiology *126*, 1151–1168.

Yekkirala, A.S., Roberson, D.P., Bean, B.P., and Woolf, C.J. (2017). Breaking barriers to novel analgesic drug development. Nat. Rev. Drug Discov. *16*, 545–564.

Zhang, H.M., Zhou, L.J., Hu, X.D., Hu, N.W., Zhang, T., and Liu, X.G. (2004). Acute nerve injury induces long-term potentiation of C-fiber evoked field potentials in spinal dorsal horn of intact rat. Sheng Li Xue Bao *56*, 591–596.

Zhao, J., Seereeram, A., Nassar, M.A., Levato, A., Pezet, S., Hathaway, G., Morenilla-Palao, C., Stirling, C., Fitzgerald, M., McMahon, S.B., et al.; London Pain Consortium (2006). Nociceptor-derived brain-derived neurotrophic factor regulates acute and inflammatory but not neuropathic pain. Mol. Cell. Neurosci. *31*, 539–548.

Zheng, L.F., Wang, R., Xu, Y.Z., Yi, X.N., Zhang, J.W., and Zeng, Z.C. (2008). Calcitonin gene-related peptide dynamics in rat dorsal root ganglia and spinal cord following different sciatic nerve injuries. Brain Res. *1187*, 20–32.

Zhong, Y., Zhou, L.J., Ren, W.J., Xin, W.J., Li, Y.Y., Zhang, T., and Liu, X.G. (2010). The direction of synaptic plasticity mediated by C-fibers in spinal dorsal horn is decided by Src-family kinases in microglia: the role of tumor necrosis factor-alpha. Brain Behav. Immun. *24*, 874–880.

Zhou, L.J., Zhong, Y., Ren, W.J., Li, Y.Y., Zhang, T., and Liu, X.G. (2008). BDNF induces late-phase LTP of C-fiber evoked field potentials in rat spinal dorsal horn. Exp. Neurol. *212*, 507–514.

Zhou, L.J., Yang, T., Wei, X., Liu, Y., Xin, W.J., Chen, Y., Pang, R.P., Zang, Y., Li, Y.Y., and Liu, X.G. (2011). Brain-derived neurotrophic factor contributes to spinal long-term potentiation and mechanical hypersensitivity by activation of spinal microglia in rat. Brain Behav. Immun. *25*, 322–334.

Zhuo, M., Wu, G., and Wu, L.J. (2011). Neuronal and microglial mechanisms of neuropathic pain. Mol. Brain *4*, 31.

STAR★METHODS

KEY RESOURCES TABLE

REAGENT or RESOURCE	SOURCE	IDENTIFIER
Antibodies		
Rabbit anti-ATF3	Santa Cruz Biotechnology	Cat# sc-188 RRID:AB_2258513
Goat anti-Iba1	Abcam	Cat# ab5076 RRID:AB_2224402
Rat anti-NIMP-R14	Santa Cruz Biotechnology	Cat# sc-59338 RRID: AB_2167795
Goat anti-CGRP	Abcam	Cat# 36001 RRID: AB_725807
Mouse anti-CGRP	Abcam	Cat# ab81887 RRID: AB_1658411
Isolectin B4-FITC	Sigma	Cat# L2895
Rabbit anti-Synaptophysin	Abcam	Cat# ab16659 RRID: AB_443419
Rabbit anti-GAP43	Abcam	Cat# ab128005 RRID:AB_11141048
Rabbit anti-Substance P receptor	EMD Millipore	Cat# AB5060 RRID:AB_2200636
Goat anti-CSF1	R&D Systems	Cat# AF416 RRID:AB_355351
Goat IgG	R&D Systerms	Cat# AB-108-C RRID:AB_354267
Rabbit anti-CSF1R	Santa Cruz Biotechnology	Cat# sc-692 RRID:AB_631025
Rat anti-CD11b	Biolegend	Cat# 101202 RRID:AB_312785
Rabbit anti-BDNF	Millipore	Cat# AB1534 RRID:AB_90746
Rabbit anti- phospho-p38	Cell Signaling Technology	Cat# 4511 RRID:AB_2139682
Mouse anti-β-actin	Cell Signaling Technology	Cat# 3700 RRID:AB_2242334
Chemicals, Peptides, and Recombinant Proteins		
D-AP5	Tocris	Cat# 0106
Lidocaine	Sigma	Cat# L7757
Collagenase	Sigma	Cat# C9891
Trypsin	Sigma	Cat# T9201
Poly-L-Lysine	Sigma	Cat# P4832
Glutamine	Sigma	Cat# G7513
ANA-12	Tocris	Cat# 4781
666-15	Tocris	Cat# 5661
SB203580	Tocris	Cat# 1202
CSF1	Biolegend	Cat# 576402
BDNF	R&D Systems	Cat# 248-BD
Tamoxifen	Sigma	Cat# T5648
Diphtheria toxin	Sigma	Cat# C8286
Urethane	Sigma	Cat# U2500
Lidocaine	Sigma	Cat# L7757
Fluoromount-G	Southern Biotech	Cat# 0100-01
Experimental Models: Organisms/Strains		
C57BL/6J	Jackson Laboratories	Cat# JAX:000664 RRID:IMSR_JAX:000664
$CX3CR1^{CreER/+}$ mice	Parkhurst et al., 2013	Cat# JAX:021160, RRID:IMSR_JAX:021160
$BDNF^{flox/flox}(BDNF^{TM3JAE}/J)$	Jackson Laboratories	Cat# JAX:004339, RRID:IMSR_JAX:004339
$R26^{iDTR/+}$ mice	Jackson Laboratories	Cat# JAX:007900, RRID:IMSR_JAX:007900
Sprague–Dawley rats	Charles River Laboratory	Cat# 10395233, RRID:RGD_10395233
Oligonucleotides		
Csf1 Forward: GTGTCAGAACACTGTAGCCAC	Thermo Fisher Scientific	N/A
Csf1 Reverse: TCAAAGGCAATCTGGCATGAAG	Thermo Fisher Scientific	N/A
β-actin Forward: CCACACCCGCCACCAGTTCG	Thermo Fisher Scientific	N/A

(*Continued on next page*)

Continued

REAGENT or RESOURCE	SOURCE	IDENTIFIER
β-actin Reverse: TACAGCCCGGGGAGCATCGT	Thermo Fisher Scientific	N/A
Software and Algorithms		
ImageJ	National Inst. Of Health	https://imagej.nih.gov/nih-image/index.html, RRID:SCR_003070
GraphPad Prism 7	GraphPad	https://www.graphpad.com/RRID:SCR_002798
OriginPro 8.0	OriginLab,	https://www.originlab.com/index.aspx?go=Products%2FOrigin, RRID:SCR_015636
LTP program	WinLTP Ltd. and The University of Bristol,	https://www.winltp.com/,RRID:SCR_008590
Other		
EVOS FL	Thermo Fisher Scientific	N/A
Zeiss LSM 510, 780, 800 META inverted confocal microscope	Carl Zeiss Microscopy GmbH, Gottingen, Germany	N/A
C2	Nikon	N/A
ImageQuant LAS4000	Fujifilm Life Science	N/A
Tecnai G^2 Spirit Twin electron microscope	FEI, Hillsboro, OR	N/A
Vibratome	MA752, Campden	N/A

CONTACT FOR REAGENT AND RESOURCE SHARING

Further information and requests for reagents may be directed to and will be fulfilled by the lead contact author, Long-Jun Wu (wu.longjun@mayo.edu).

EXPERIMENTAL MODEL AND SUBJECT DETAILS

Animals and husbandry

Young adult (8-12 weeks old) C57BL/6 (Charles River) mice were used as wild-type controls. In some experiments, Sprague–Dawley rats (210–280 g, Laboratory animal center, Sun Yat-sen University, Guangzhou) were used. $CX3CR1^{CreER/+}$ mice (gifted from Dr. Wen-Biao Gan at New York University) were crossed with $R26^{iDTR/+}$ (Jackson Laboratory) to obtain $CX3CR1^{CreER/+}$:$R26^{iDTR/+}$ mice. $CX3CR1^{CreER/+}$ mice were crossed with $BDNF^{flox/flox}$ ($BDNF^{TM3JAE}$/J, Jackson Laboratory) to obtain $CX3CR1^{CreER/+}$:$BDNF^{flox/flox}$ mice. Most experiments were performed with adult male mice, and only in one special experiment of sex differences, male and female mice was used, which was specially indicated. The rodents were housed in a standard 12 h light/dark cycle (lights on 06:00) and temperature (23 ± 2°C) controlled room with access to food and water *ad libitum*. All experimental protocols and animal handling procedures were approved by the institutional animal care and use committee at Rutgers University (USA) or Sun Yat-sen University (China).

Electrical stimulation-induced chronic pain model

Rodent were anesthetized with 2% isoflurane anesthesia and the left sciatic nerves were dissected free for electrical stimulation with bipolar platinum hook electrodes. HFS at different intensities (1, 10, 20 V) was delivered to the left sciatic nerve. In the sham group, the sciatic nerve was exposed and the electrode was laid aside without electrical stimulation. At the end, the muscle and skin were closed in two layers. Following surgery, mice were allowed to awake from anesthesia and were fully mobile before being returned to their home cage. The surgery was always performed in littermates and housed together until further experimentation.

Spared nerve injury

Spared nerve injury (SNI) surgery was performed as previously described (Decosterd and Woolf, 2000). Under 2% isoflurane anesthesia, incision was made along the mid-line of the left hind limb. The common peroneal and the tibial nerves were then ligated and cut (2 mm sections removed), but the sural nerve was left intact. At the end, the wound was sutured in two layers.

METHOD DETAILS

Microglia ablation and repopulation

According to the method described in our recent study (Peng et al., 2016), $CX3CR1^{CreER/+}$ (Control) mice or $CX3CR1^{CreER/+}$:$R26^{iDTR/+}$ mice (over 6 weeks old) were intraperitoneally (i.p.) given tamoxifen (TM, Sigma, T5648, 0.15 g/kg, 20 mg/ml in corn oil with

ultrasound) every other day for 4 times. Then two doses of diphtheria toxin (DT, Sigma, C8286, 50 μg/kg, 2.5 μg/ml in PBS) or vehicle (corn oil) were i.p. injected 3 weeks later to induce microglial ablation. To test the role of microglial ablation or repopulation or the effect of TM only, HFS-induced synaptic plasticity and chronic pain, HFS was delivered to the sciatic nerve on the 3rd or 21st day after the first DT injection, or the 7th day before the first DT injection, respectively. The effectiveness of microglial ablation or repopulation was tested at these time points by performing immunostaining of Iba1 in the spinal cord tissue.

Microglial BDNF deletion

$CX3CR1^{CreER/+}$:$BDNF^{flox/flox}$ mice were i.p. treated with TM (0.15 g/kg, 20 mg/ml) or vehicle (corn oil) 3 times every other day and then kept for more than 3 weeks to be used as microglial BDNF ablation ($BDNF^{-/-}$) mice. The mice without injection of TM served as control group ($BDNF^{+/+}$).

In vivo extracellular recordings in the dorsal horn

Protocols for surgical preparation and *in vivo* extracellular recordings of the C-fiber-induced field potential have been described in our previous studies (Liu and Sandkühler, 1995; Zhong et al., 2010). Briefly, animals were anesthetized with urethane (Sigma, 1.5 g/kg, i.p.). A laminectomy was performed to expose the lumbar enlargement of the spinal cord. The left sciatic nerve was gently dissected free for electrical stimulation with a bipolar platinum hook electrode. Then the animal were placed in a stereotaxic frame and a small well with gel seal was formed on the cord dorsum at the recording segments for drug application or warm paraffin oil. The dura mater was incised longitudinally. Then, test stimuli (0.5 ms duration, every 1 min, at C-fiber intensity) was delivered to the sciatic nerve. C-fiber evoked fEPSP was recorded from the dorsal horn of mouse spinal cord with a glass microelectrode (filled with 0.5 M sodium acetate, impedance 0.5–1 MΩ). The optimal recording position for C-fiber fEPSP was at a depth of around 200–350 μm from the surface of the L4 lumbar enlargement of the spinal cord for mice. An A/D converter card (National Instruments M-Series PCI express) was used to digitize and store data at a sampling rate of 10 kHz in a computer. fEPSP was at a depth of around 2 of C-fiber evoked fEPSP was determined on-line by LTP program (https://www.winltp.com/). In each experiment, amplitudes of five consecutive fEPSP recorded at 1 min intervals was averaged. The mean amplitudes of the responses before 0.1 M PBS/saline or drug application served as baseline. Different intensities (1, 10, 20 V) of high-frequency stimulation (HFS: 100 Hz, 0.5 ms, 100 pulses given in 4 trains of 1 s duration at 10 s intervals) were used as conditional stimulation in left sciatic nerve to induce LTP of C-fiber evoked fEPSP. In some experiments to observe the effects of the drugs on C-fiber evoked field potentials, goat anti-CSF1 antibody (AF416, 40.0 ng/μl, 20 μl, R&D Systerms, USA) or normal goat IgG control (AB-108-C, 40.0 ng/μl, R&D Systerms, USA) was directly administered onto the spinal dorsal surface at the recording segments 30 min after stable recording of C-fiber evoked field potentials. Only one experiment was performed in each animal. At the end of the experiment, the animals were decapitated under anesthesia.

Behavioral tests

Mechanical Test

Each mouse/rat was acclimated to the test environment and the experimenter 3 days prior to HFS and sham operation and was again allowed to acclimate for about 30 min before the behavioral test. All the tests were performed by two experimenters, one blinded to drug and/or surgery treatments. To test mechanical allodynia, animals were placed on an elevated wire grid and the plantar surface of the paw was stimulated with a set of Von Frey filaments (0.04 – 2 g for mice and 0.4 – 25 g for rats; North Coast medical). Each filament was applied from underneath the metal mesh floor to the lateral and medial plantar surface of the paw. The positive response of mechanical allodynia was considered to be a brisk filament evoked withdrawal response for up to 3 s to at least one of five repetitive stimuli. 50% paw withdrawal threshold (PWT) was determined using the up-down method. Mice with pre- surgery/treatment basal mechanical response threshold equal to or less than 0.16 g were excluded for use.

Thermal Test

Thermal hypersensitivity was measured using a plantar test (7370, UgoBasile, Comeria, Italy) according to the method described by Hargreaves et al. (1988). The center plantar surface of the hind paw was exposed to a beam of radiant heat through a transparent Perspex surface. The paw withdrawal latency (PWL) was recorded when a withdrawal response to the radiant heat was observed. The basal PWL of normal adult C57BL/6J mice was 9-12 s, with a cutoff of 20 s to prevent tissue damage. The heat stimulation was repeated 4 times at an interval of 5-6 min for each paw and the mean calculated.

Rotarod test

The rotarod tests were performed as an index of injury-induced motor deficits by a five-lane Rotarod apparatus (Med Associates Inc). The rotarod speed started from 4 rounds per minute (RPM) and uniformly accelerated to 40 RPM in 5 minutes. Only the latency to fall off the rotating rod was recorded. Each mouse was tested for 3 trials with 15 min interval. There is no training prior to the test phase.

Local application of lidocaine around the sciatic nerve

Two percent lidocaine (L7757, 50 μl, Sigma) was administered around the stimulated sciatic nerve 15 min before HFS to block nociceptive nerve transmission via inhibition of sodium channels.

Intrathecal injection of drugs

Adult male mice (20–30 g) were anesthetized with 1.5% isoflurane and injected intrathecally with different drugs in a volume of 5.0 μL with a luer-tipped Hamilton syringe at the level of the pelvic girdle. The drugs included goat anti-CSF1 antibody (AF416, 40.0 ng/μl, R&D Systerms, USA), normal goat IgG control (AB-108-C, 40.0 ng/μl, R&D Systerms, USA), recombinant mouse CSF1 (576402, 6 ng/μl, Biolegend), recombinant mouse BDNF (248-BD, 20 ng/μl, R&D systems), D-AP5 (0106, 50 μg/ml, Tocris) or vehicle (0.1 M PBS).

Fluorescent immunohistochemical staining

After mice were anesthetized with isoflurane (5% in O_2), they were perfused intracardially with 20 mL PBS followed by 20 mL of cold 4% paraformaldehyde (PFA) in PBS (pH 7.4) containing 1.5% picric acid. The electrical stimulated site of the ipsilateral sciatic nerve in HFS group or the proximal stump of sciatic nerve in SNI group before entering the popliteal fossa were used for studying nerve damage. L4 dorsal root ganglion (L4 DRG) and L3–L5 segments of spinal cord were harvested and post-fixed in the same fixative for 4–6 hours, then replaced with 30% sucrose in PBS overnight at 4°C. All the tissues were sliced into 15 μm sections using a cryotome (Leica CM1250, Germany) and transferred on to Superfrost Plus Microscope slides (Fisherbrand®).

For cultured spinal slice immunostaining, the slices were fixed with 4% PFA (Sigma) for 30 mins and then washed in Tris-buffered saline (TBS, pH 7.3) for 3 times with 5-min interval. The tissue sections/cultured DRG neurons were first blocked with 5% donkey serum in 0.3% Triton X-100 (Sigma) for 60/30 min at room temperature (RT), and then incubated overnight at 4°C with a mixture of rabbit anti-ATF3 (1:500, sc-188, Santa Cruz Biotechnology, USA), mouse anti-CGRP antibody [4901] (1:2000, ab81887, Abcam, USA), isolectin B4-FITC (1:100, L2895, Sigma, USA), rabbit anti-GAP43 antibody (1:500, ab128005, Abcam, USA), rabbit anti-Substance P receptor antibody (1:500, AB5060, Millipore, USA.), rabbit anti-Iba1 (1:2000, 019-19741, Wako), goat anti-M-CSF antibody (1:500, AF416, R&D Systems, USA); rat anti-CD11b (1:500, 101202, Biolegend, USA); goat anti-Iba1 (1:500, ab5076, Abcam, USA) or rabbit anti-CSF1R (1:500, sc-692, Santa Cruz Biotechnology, USA). Subsequently, the sections were then incubated with secondary antibodies (Alexa Fluor® 488, 555, 647; Life Technologies) for 60-90 min at RT. The coverslips were mounted with Fluoromount-G (Southern Biotech) and fluorescent images were obtained with a normal microscope (EVOS FL) (Thermo Fisher Scientific), and confocal microscopes (LSM510, 780, 800, Zeiss, C2, Nikon). For cultured spinal cord slice, the confocal images were taken 50 μm thick at depth up ~50 μm from the slice surface.

Western blot

Under isoflurane anesthesia, ipsilateral L4-5 spinal dorsal horn tissue was isolated and homogenized with protease inhibitor cocktail (Roche Molecular Biochemicals) and phosphatase inhibitor. Equal concentration of protein samples were resolved on 4%–12% NuPAGE® Bis-Tris Precast Gels (Thermo Fisher Scientific), and then transferred to PVDF membranes (iBlot® 2 Transfer Stacks, PVDF, regular size (Novex) (Thermo Fisher Scientific). Membranes were blocked and then probed with primary antibodies: rabbit anti-Iba1 (1:2000, 016-20001, Wako); mouse anti-CGRP antibody [4901] (1:5000, ab81887, Abcam, USA), rabbit anti-CSF1R (1:1000, sc-692, Santa Cruz Biotechnology, USA), rabbit anti-BDNF (1:1000, AB1534, Millipore, USA), goat anti-M-CSF antibody (1:1000, AF416, R&D Systems, USA); rabbit anti-p-p38 (1:2000, #4511, Cell Signaling Technology, USA), mouse anti-β-actin (1:5000, #3700, Cell Signaling Technology, USA) overnight at 4°C. After washed, membranes were then incubated with an HRP-conjugated secondary antibody (1:5000~8000, Jackson Immune Laboratory) at RT for 90 min. Protein bands were detected by ECL detection reagent (34095, Thermo Fisher Scientific) and captured on ImageQuant™LAS4000 (Fujifilm Life Science). Integrated optical density was determined using ImageJ 1.48 (NIH). Standard curves were constructed to establish that we operated within the linear range of the detection method.

Ultrastructure of rat sciatic nerves

After pain behavioral tests at the 7 days after sham, HFS or SNI, the left sciatic nerves of rats (n = 2-3 rats/group, 2 mm distal to the stimulated or injury point) were obtained and fixed in 4% glutaraldehyde and post-fixed in 1% osmium tetroxide solution at 4 °C. These samples were then dehydrated in graded ethanol series and embedded in Spurr's resin between two slides coated with dimethyldichlorosilane (Sigma) in a 37°C degree oven for 2 hours and then placed in 60°C for 48 hours. The sciatic nerve sections (70 nm) were prepared, then observed and imaged with Tecnai G^2 Spirit Twin electron microscope (FEI, Hillsboro, OR).

Pre-embedding immunoelectron microscopy (IEM)

A total of 5 male C57BL/6J mice (sham: n = 2 mice, HFS 7d: n = 3 mice) at 8-week-old were used. Animals were anesthetized with 7.5% chloral hydrate (1.0 g/kg, i.p.) and perfused with 0.1 M phosphate-buffered saline (PBS, pH 7.2) for 1-2 min and then followed by 150 mL fixative solution for about 30 min. The fixative solution was consisted of 0.1% glutaraldehyde, 4% paraformaldehyde and 15% saturated picric acid in 0.1 M phosphate buffer (PB, pH 7.2). The lumbar enlargement of spinal cord was harvested and post-fixed in the same fixative solution but without glutaraldehyde for 3 h at 4°C. Spinal transverse sections were cut at a thickness of 50 μm on a vibratome and then stained using DAB immunohistochemistry method. After washed in PB and rinsed in 25% sucrose PB solution for 30 min, the sections were dipped in liquid nitrogen for 2 s and quickly rinsed in 0.05M Tris-buffered saline (TBS, pH 7.2) for 5 min then incubated in 20% donkey serum in TBS for 30 min. After overnight incubation at 4°C with goat anti-CGRP antibodies (Abcam, 1:150) in 2% donkey serum TBS solution, the spinal sections were then incubated at 4°C with biotin labeled donkey

anti-goat antibodies diluted 1:100 in 2% donkey serum TBS solution overnight. Slices were incubated with HRP-Streptavidin (PK-6101, Vectorlabs) for 4 hours at room temperature and then treated with diaminobenzidine (DAB, SK-4100, Vectorlabs) and H_2O_2. After being rinsed in PB for 5 min three times, the slices were treated with 1% osmic acid in PB, dehydrated in 50% alcohol and dipped in 1% saturated uranyl acetate (70% alcohol solution) for 40 min. Then the sections were dehydrated in increasing concentrations of ethanol and embedded in Spurr's resin between two slides coated with dimethyldichlorosilane (Sigma) in a 37°C degree oven for 2 hours and then placed in 60°C for 48 hours. Selected sections were cut and reconstructed with a blade and recut into serial ultrathin sections. To avoid the effect of densely stained myelinated axons on CGRP immunoreactivity, the sections were not incubated in lead citrate. These ultrathin sections (70 nm) were collected on 200-mesh copper grids for examination with a Tecnai G^2 Spirit Twin electron microscope (FEI, Hillsboro, OR).

qRT-PCR

L4-5 DRGs were excised from each mouse and homogenized in TriZol. RNA was isolated using TriZol/chloroform extraction and cDNA was prepared from total RNA by reverse transcription reaction with PrimeScript RT Master Mix (RR036A, Takara). qRT-PCR was performed with CFX 96 touch3 (Bio-rad) using TB Green premix Ex Taq (RR820A, Takara). The conditions for fast qRT-PCR were as follows: 1 cycle of 95°C for 30 s, 40 cycles of 95°C for 5 s, and 60°C for 30 s. At the end of the PCR, the samples were subjected to melting analysis to confirm amplicon specificity. Primers sequences are listed as follow: CSF1 Forward (5′-GTGTCAGAACACTGTAGCCAC-3′), CSF1 Reverse (5′-TCAAAGGCAATCTGGCATGAAG-3′); β-actin forward (5′-CCACACC CGCCACCAGTTCG-3′), β-actin reverse (5′-TACAGCCCGGGGAGCATCGT-3′). The relative CSF1 mRNA expression was were normalized to β-actin in the same group. The ratio of protein/β-actin from sham group were set as 1 baseline. The data from other groups show the fold with sham baseline.

Culture of DRG neurons

C57BL/6 mice (4∼6wold) were made unconscious by CO_2 and then decapitated immediately. After that, the DRGs were bilaterally dissected out and transferred to DMEM/F12 (GIBCO). After DRGs were digested with 5 mL collagenase (3 mg, C9891 sigma) and trypsin (2 mg, T9201, sigma) mixture solution for 25 min, and the same volume of complete medium (DMED/F12 + 10% FBS + 1% penicillin and streptomycin 100 ×, GIBCO) was added to stop the digestion. Single DRG cells were obtained. These cells were cultured in 0.01% PLL-coated (Poly-L-Lysine, P4832, sigma) 48well plates in cell culture medium: DMEM/F12 + 10% FBS + 1% penicillin and streptomycin + 1% glutamine (200 mM, G7513, sigma). Four hours later, the supernatant was carefully discarded, and new culture medium was added. Culture for 4 days and the cell can be treated for following experience: BDNF group contained 50 μg/ml recombinant mouse BDNF (248-BD, R&D systems); ANA-12 group contained 10 or 50 μM ANA-12 (a low-molecular weight TrkB antagonist, Tocris), ANA-12 + CSF1 group was cultured with 10 or 50 μM ANA-12 1 h prior to BDNF, 0.5 μM 666-15 (a potent and selective CREB inhibitor, Tocris), 666-15 + CSF1 group was cultured with 0.5 μM 666-15) 1 h prior to BDNF; KCl group contained 40 mM KCl. Then DRG neurons were cultured in humid conditions and 5% CO_2 at 37°C. At 24 hours after BDNF, KCl or vehicle (0.02% DMSO), the culture media were harvested for western blot (WB) to show CSF1 release and the DRG neurons were fixed for CGRP immunofluorescence.

Acute spinal cord slice culture

The acute spinal cord slice culture was performed following the procedures described previously (Liu et al., 2017). Briefly, normal 4∼6-week-old C57BL/6 mice were anesthetized with 10% urethane (1.5 g/kg, Sigma), then were plunged into 75% alcohol solution for 30 s. The spines were isolated quickly and put into 4°C precooled slice cutting buffer (2.5% 1 M HEPES in EBSS, Sigma). Under aseptic conditions, the transverse lumbar spinal cord slices were cut at 400 μm thickness with a vibratome (MA752, Campden) and then transferred onto 0.4 μm culture inserts (PIHP03050, Millipore) which were pre-equilibrated with 1 mL of culture medium. All culture media contained 50% MEM (GIBCO), 25% EBSS (Sigma), 25% horse serum (GIBCO), 6.5 mg/ml glucose (Sigma), 1% penicillin-streptomycin and 0.05% DMSO (Sigma). CSF1 group contained 1 μg/ml CSF1 (576406, BioLegend); SB203580 (Sigma) group contained 1 or 10 μM SB203580 (a selective inhibitor of p38 MAPK, Tocris), SB203580 + CSF1 group was cultured with 1 or 10 μM SB203580 1 h prior to CSF1. The spinal cord slices were cultured in humid conditions and 5% CO_2 at 37°C. At 6 hours after CSF1 or vehicle (0.02% DMSO), the spinal cord slices were collected for immunofluorescence or WB, and the culture media were harvested for WB to show BDNF release.

QUANTIFICATION AND STATISTICAL ANALYSIS

Statistical analysis

Data were presented as mean ± SEM. Unpaired Student's t test (2 tailed) were performed after confirming that the groups were normally distributed with equal variances. Pain behavior tests and electrophysiological data were analyzed by two-way repeated ANOVA, followed by individual post hoc comparisons (post hoc Tukey's test or Fisher's) to establish significance. Other changes of values of each experimental group were tested using one-way ANOVA, followed by individual post hoc comparisons (post hoc Tukey's or Fisher's test). Statistical significance was calculated using software OriginPro8.0 (OriginLab, USA). Level of significance is indicated with *or $^{\#}p < 0.05$, ** or $^{\#\#}p < 0.01$, *** or $^{\#\#\#}p < 0.001$.

Quantification of immunofluorescence staining

For the analysis of ATF3 or CGRP-positive cells in the DRGs, the DRG neurons was identified by adjusting brightness/contrast and all neuronal cells with a clear nuclear profile were counted using the ImageJ image processing and analysis program. 2-4 sections of L4 DRG from each animal were chosen at random with the group blinded. The percentage of ATF3 or CGRP-positive neurons in the DRG neurons was then calculated (Flatters and Bennett, 2006; Matsuura et al., 2013).

Fluorescent signal intensity was also quantified using relative optical density (RelOD) by ImageJ software (National Institutes of Health, Bethesda, MD). Images used for quantification represent serial optical sections obtained along the z axis (z stacks), using 25X, 40X, 63X plan-apochromatic water-immersion objective. For an unbiased representation of the images taken, all the parameters of laser power, pinhole size and image detection were kept constant for all samples. Based on Rexed laminae of the spinal cord, the analysis criteria of CGRP-immunoreactivity (IR) fibers density in the superficial layer is shown in Figure 2C.The criteria of identification and quantification of the density of CGRP-positive boutons per lamina have been described in previous publications(Saeed and Ribeiro-da-Silva, 2012). Briefly, the fluorescent CGRP intensity in layer I and IIo, IIi and III & IV was respectively calculated and the intensity in layer I and IIo from WT sham tissues or control group was set as the 100% baseline. The RelOD of other protein expression was also measured by the same method. The intensity in L4 DRG from sham tissues or control group was set as the 100% baseline. The data from each of the other groups were normalized and compared with baseline. Three to five sections per mouse from 3-4 mice were randomly selected for each group.

TEM analysis

According to the Erlanger-Gasser Classification, peripheral nerve fibers are grouped based on the diameter of an axon: Aα (13-20 μm); Aβ (6-12 μm); Aδ (1-5 μm); C (< 1.5 μm). The diameters of myelinated axons were calculated on the total surface of the semithin sections of sciatic nerves using the g-ratio calculator plug-in developed for ImageJ software. Axons and nerve fibers were grouped into increasing size categories separated by 1 μm to calculate their distribution. The G ratios were measured as ratios of the axon diameter to the fiber diameter in equivalent 26 × 17 μm areas from each nerves previously described (Bangratz et al., 2012; Chen et al., 2015). Data for this study were collected from total of 4-6 micrographs of sciatic nerve fiber TEM cross-sections from 2-3 rats/group.

IEM analysis

Lamina II was identified by the paucity of myelinated fibers within the neuropil, which facilitated the determination of the laminae I/II, IIi and III/IV borders of the dorsal horn of the spinal cord when sections were observed in electron microscopes. Data for this study were collected from a total of 36 micrographs (2-3 micrographs/layer/mouse) of cross-sections of well-preserved $CGRP^+$ immunoreactive elements from five animals. Measurements of labeled structures were made on electron micrograph negatives at 13,500-37,000 × magnification using a measuring magnifier calibrated in 0.2 mm gradations. Measurements of the number of CGRP positive ($CGRP^+$) varicosities (Figure 2e, in black circles) or synapses (arrows) in the different layers between sham and HFS 7d groups were made by two experimenters who were blinded to the treatment.

Analysis of CGRP neurite length

The analyses of CGRP neurite lengths of cultured DRG neurons were determined on ImageJ software following the procedures described by Jun et al. (2015). The largely overlapped CGRP -positive ($CGRP^+$) neurons were excluded to estimate. Using the NeuronJ plug-in, all the neurite length of $CGRP^+$ DRG was measured, the average value calculated for 3-4 neurons of each image (20 X), and the mean neurite length derived from the 4-8 images average values per group (> 15 neurons/group). Neurites were traced manually from the soma outward, excluding those < 5 μm. All quantitative data were obtained by a blinded experimenter and normalized to the WT control.